CHALMERS

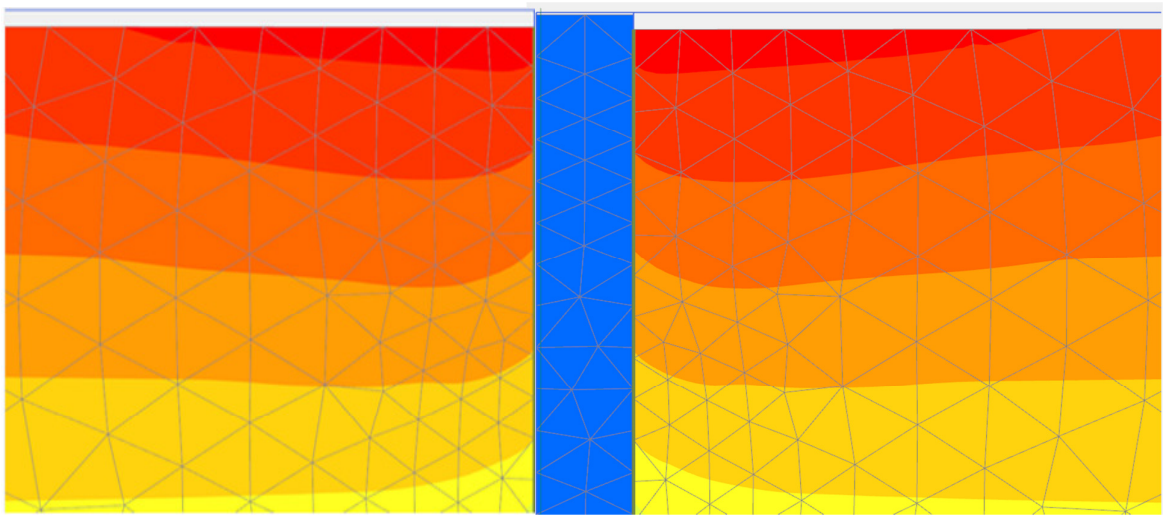

Modelling of negative skin friction on bored piles in clay

Master of Science Thesis in the Master's Programme Infrastructure and Environmental Engineering

NELSON KIPROTICH

Department of Civil and Environmental Engineering
Division of GeoEngineering
Geotechnical Engineering
CHALMERS UNIVERSITY OF TECHNOLOGY
Göteborg, Sweden 2015

Master's Thesis 2015:38

MASTER'S THESIS 2015:38

Modelling of negative skin friction on bored piles in clay

Master *of Science Thesis in the Master's Programme*

Infrastructure and Environmental Engineering

Department of Civil and Environmental Engineering
Division of GeoEngineering
Geotechnical Engineering
CHALMERS UNIVERSITY OF TECHNOLOGY
Göteborg, Sweden 2015

Modelling of negative skin friction on bored piles in clay

Master of Science Thesis in the Master's Programme Infrastructure and environmental Engineering

© NELSON KIPROTICH, 2015

Examensarbete / Institutionen för bygg- och miljöteknik,
Chalmers tekniska högskola 2015:38

Department of Civil and Environmental Engineering
Division of GeoEngineering
Geotechnical Engineering
Chalmers University of Technology
SE-412 96 Göteborg
Sweden
Telephone: + 46 (0)31-772 1000

Cover:
Image output from PLAXIS finite elements software showing a pile and deformed soil.

Chalmers Reproservice
Sweden 2015

Modelling of negative skin friction on bored piles in clay

Master of Science Thesis in the Master's Programme Infrastructure and Environmental Engineering

NELSON KIPROTICH

Department of Civil and Environmental Engineering
Division of GeoEngineering
Geotechnical Engineering
Chalmers University of Technology

ABSTRACT

Negative skin friction is a problem that occurs in a pile foundation if the soil settles more than a pile. The settling soil adds an extra load on the pile by mobilizing shear at the pile-soil interface. Most of the analysis is carried out using conservative approaches such as α and β methods. In this thesis, an investigation is carried out on finite elements modelling of a pile subjected to negative skin friction due to the lowering of the groundwater table. The study has been carried out using the finite elements software PLAXIS 2D. First, an evaluation of the PLAXIS 2D soil structure interface is carried out, and thereafter an axisymmetric numerical model of a bored pile is developed to analyse a documented centrifuge pile test. A consolidation analysis is carried out in which the pile and the soil are modelled as volume elements. The numerical simulation overpredicted the measured maximum drag load by 17% while the ground settlements were underestimated by 35%. The skin friction, drag loads, and α-factor increase with time due to consolidation after lowering of the groundwater level. A maximum α-factor of 0.6 is obtained at the end of the test. Estimation with the Swedish code of practice which recommends an α-factor 0.7 for long-term undrained calculations exceeds the measured maximum drag load by 76%. Advanced numerical analysis has been recommended for pile projects where an optimized solution results in savings over result obtained from other simpler methods.

Key words: Negative skin friction, drag load, groundwater, finite elements, pile foundation

Contents

1 INTRODUCTION 1

1.1 Problem 1

1.2 Objectives 1

1.3 Scope and limitations 2

2 LITERATURE REVIEW 3

2.1 The concept of negative skin friction 3

2.1.1 Neutral point 3

2.1.2 Relative pile-soil settlements 4

2.2 Analytical and empirical methods of analysing NSF 5

2.2.1 The α-method 5

2.2.2 The β-method 6

2.2.3 The λ-method 7

2.2.4 Geotechnical end bearing capacity 7

2.2.5 In situ tests 8

2.3 Numerical methods 10

2.3.1 Load transfer method 10

2.3.2 Finite elements method (FEM) 11

2.4 Finite elements analysis and PLAXIS 11

2.4.1 Linear elastic model 12

2.4.2 Interface constitutive model 12

2.4.3 Constitutive soil model 12

3 METHODOLOGY 15

3.1 Modelling a pile in PLAXIS 2D 15

3.1.1 PLAXIS soil structure interface 15

3.2 Case study: A centrifuge model pile test 17

3.2.1 Laboratory centrifuge test 18

3.2.2 Soil and pile properties 20

3.2.3 Test setup 21

3.2.4 Numerical model in PLAXIS 22

4 RESULT 25

4.1 The base as infinitely stiff 25

4.1.1 Vertical effective stresses 25

4.1.2 Ground and pile head settlements 26

4.1.3 Axial load distribution 27

4.2 Modelling with an elastic drainage sand layer 29
4.2.1 Ground and pile head settlements 29
4.2.2 Skin friction 31
4.2.3 Axial load distribution 31
4.2.4 Pile-soil settlements in Plaxis 33
4.2.5 Excess pore water pressure 34
4.2.6 The α-factor 35
4.3 Parameter study 36
4.3.1 Interface strength 36
4.3.2 Pile stiffness 36
4.3.3 Pile diameter 37
4.3.4 Axial loads 38
4.4 Discussion 39

5 CONCLUSION AND RECOMMENDATIONS 41
5.1 Conclusion 41
5.2 Recommendations for future work 42

REFERENCES 43

APPENDICES 45
Appendix A1: Interface (plastic analysis) 45
Appendix A2: Interface plastic and consolidation analysis 49
Appendix A3: Estimating the initial void ratio 50
Appendix A4: OCR and undrained shear strength 51
Appendix A5: Final soil settlement profiles 52

Preface

In this study, an investigation of 2D numerical analysis of a pile subjected to negative skin friction due to consolidating soft soil has been carried out. The research has been done between January 2015 and May 2015 at the Department of Civil and Environmental Engineering at Chalmers and with the company ELU AB. The thesis was initiated by Lars Hall and Fredrick Olsson at Geotechnical section of ELU.

This project has been carried out under supervision of Dr. Jelke Dijkstra (Chalmers supervisor/examiner) and Therese Hedman (ELU supervisor), who I appreciate for their insightful guidance and support. I also give gratitude to the lecturers and colleague students for the many occasions where we shared ideas and engaged one another during the master's study period, and to the staff at ELU for their co-operation and involvement during the research. I also give my sincere thanks to the Swedish Institute for sponsorship through the master's programme. Finally, I thank my family for the patience and love throughout the study.

Göteborg June 2015

Nelson Kiprotich

Notations

σ	Total stress
ε	Total strain
ε^e	Elastic strains
ε^p	Plastic strains
σ_3	Minor principal stress
σ_1	Major principal stress
P_c	Preconsolidation pressure
δ	Interface friction angle
Ψ	Dilatancy angle
ϕ	Internal friction angle
τ	Shear stress
τ_{max}	Maximum shear stress
c_a	Adhesion factor
σ_n	Normal stress
R_{int}	Interface strength reduction factor
G	Gravitational acceleration

List of abbreviations

FEM	Finite Elements Method
CPT	Cone Penetration Test
OCR	Over Consolidation Ratio
NSF	Negative Skin Friction
POP	Pre Overburden Pressure

1 INTRODUCTION

Piles are slender structural elements that transmit the weight of a superstructure through weak compressible soils or water to stronger materials such as stiff soil or rock.

Piles normally support the weight of a structure and external loads either by compression or tension. In certain situations, piles may also be subjected to an extra load from the surrounding soil due to negative skin friction. This frictional force is mobilized at the pile-soil interface if the soil settles more than a pile. Extra load from negative skin friction may cause failure of a structure supported on piles and therefore it has to be considered in pile design (Davison, 1993).

The analysis of negative skin friction on piles may be accomplished through conventional empirical methods or numerical methods such as finite elements method. Progress in computer technology and geotechnical numerical modelling methods have made it possible to simulate more realistic soil properties and soil-structure interaction.

In this investigation, a numerical analyses of a pile subjected to negative skin friction due to consolidating soil is carried out. In the study, an experimental laboratory pile centrifuge test is used as a reference for the analysis. This is motivated by the fact that the test is done in a controlled laboratory condition. In the test, most of the boundary conditions are known and due to the short test duration, creep is minimized. Moreover, because the pile is installed as a bored pile, then the effects of pile installation are small. This makes the test an ideal basic case for modelling the effects of negative skin friction problem using numerical methods.

1.1 Problem

Analysis of negative skin friction on pile foundations has typically been based on empirical and semi-empirical methods. Numerical methods offer an alternative solution to analyse pile foundation problems in a more comprehensive way. In this study, an investigation of numerical analysis of negative skin friction on a pile foundation will be carried out.

1.2 Objectives

The following are the objectives:-

i. To model a pile test so as to evaluate a numerical model and method of analysis.

ii. To compare the results of skin friction computed numerically with that estimated with existing empirical methods.

iii. To carry out a parameter study on a pile subjected to negative skin friction in order to study the influence of selected design factors on negative skin friction.

1.3 Scope and limitations

The study is carried out on a single, bored, circular, end bearing, concrete pile in a 2D axisymmetric condition. The cause of negative skin friction is consolidation of a soft soil layer due to the lowering of the groundwater table. The long-term effects of creep in soft soil are not considered. PLAXIS 2D software and Soft Soil model is be used as the numerical tool for modelling the pile foundation. This is contrary to the reality since piles are 3D structures, thus modelling in 2D is a simplification.

2 Literature review

This chapter gives an introduction into negative skin friction (NSF) and the various methods of analysing it.

2.1 The concept of negative skin friction

Negative skin friction occurs when the soil settles more than the pile. Its main cause is consolidation of soft soil due to placement of surcharge, lowering of the groundwater table and soil reconsolidation after pile driving. It can also occur in nearly incompressible cohesionless material such as gravel that overlies consolidating soft clays. Consolidation increases soil effective stresses which increase pile shaft friction (Fellenius, 2006). Another reported cause is compaction due to ground vibration (Davison, 1993). The magnitude of negative skin friction developed on a pile depends on the relative movement between the soil layers and the pile shaft, the elastic compression of the pile and the rate of consolidation of compressible soil layers (Fellenius, 2006).

2.1.1 Neutral point

The settlement of a pile due to skin friction eventually leads to equilibrium where the upper soil layers exert a downward force while the lower layers exert an upward force on the pile. The location of the transition between negative shear and positive shear is referred to as the neutral plane (see Figure 2.1). It is also the location of no relative movement between the pile and the soil and the point where the pile experiences maximum load. The location of the neutral plane depends on the amount of pile toe penetration (Fellenius, 2006). In end bearing piles, the neutral plane is located small distance above the bedrock surface while for floating piles; it is located above the pile toe. With stiff soil such as sand or weakened rock, small relative pile-soil movements shift the neutral plane slightly above the pile toe.

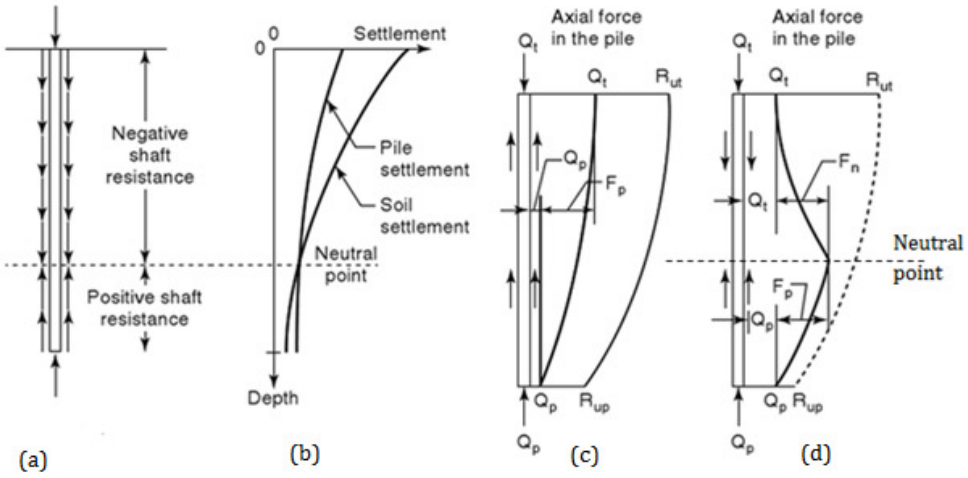

Figure 2.1: Illustration of (a) Neutral plane, (b) pile-soil settlements, (c) pile without negative skin friction (d) pile with negative skin friction (Briaud, 2013)

Negative skin friction causes drag load that increases pile stresses and additional pile settlement (i.e. down drag). As a result, negative skin friction may lead to a serviceability failure due to excessive settlements in shaft bearing piles or structural failure in end bearing piles. In most cases of piles with drag loads, the serviceability criterion governs the design (Briaud, 2013).

2.1.2 Relative pile-soil settlements

The amount of relative pile soil movements to attain full skin friction is estimated at 0.3 to 1% of pile diameter. On the other hand, the base resistance requires larger displacements in the order of 10 to 20% of pile tip diameter to generate full friction (Tomlinson & Woodward, 2008). Full toe resistance may not be accounted for on piles in soft cohesive and cohesionless soils as the foundation will have failed due to excessive settlement at the moment full toe resistance is achieved (see Figure 2.2, where S is settlement, S_{sg} is the ultimate settlement, R_b is the base resistance, R_s is the shaft resistance, and R is the combined toe and shaft resistance).

In a field pile test carried out at Bäckebol, Sweden with a pile of diameter 300 mm and 55 m long, large drag loads were measured as a result of very small soil settlements of 2 mm (Fellenius, 2006). Observations were also made from application of temporary axial loads on the pile head that lead to pile settlements. These pile settlements generated positive shaft resistance and reduced negative skin friction.

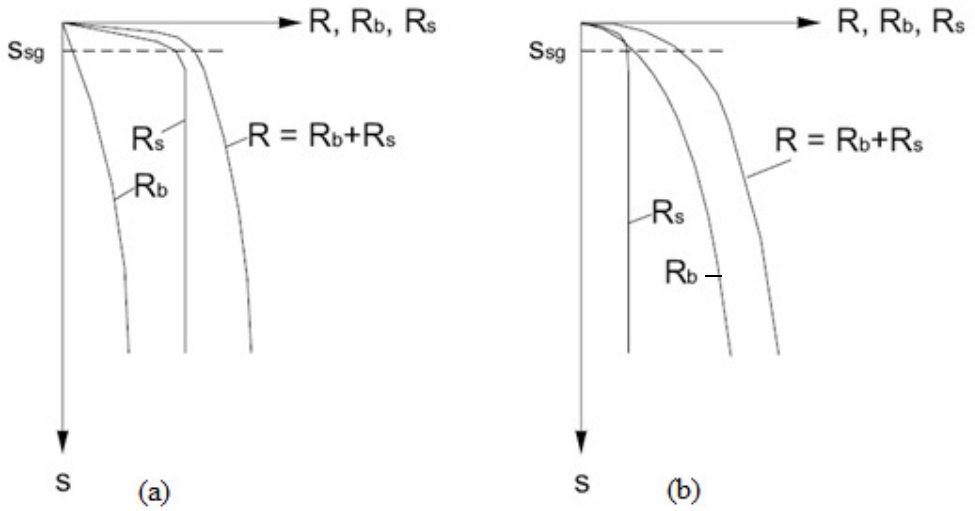

Figure 2.2: Load-settlement curves for (a) shaft bearing and (b) point bearing piles (Kempfert & Gebreselassie, 2006)

2.2 Analytical and empirical methods of analysing NSF

Empirical methods include (α, cone penetration test (CPT) and analytical (β). Analytical and empirical methods of calculating skin friction use either total or effective stress principle. Both approaches are widely used, however the effective stress methods are a more realistic approach since the soil strength is based on effective stresses (Fellenius (2006)). For clays, the difficulty to predict excess pore water pressure makes the use of undrained shear parameters more appropriate for estimating the short term shear strength (Kempfert & Gebreselassie, 2006).

2.2.1 The α-method

The α-method is an empirical method that is given by Equation 2.1 (Bowles, 1997):

$$f_s = \alpha . c_u \qquad (2.1)$$

where α is adhesion factor. This factor depends on the strength of the soil, the pile properties and time after pile installation. It typically ranges between 0.3-1 for bored piles; and between 1-1.5 for displacement piles but may be higher in stiff clays (Kezdi & Rethati, 1988).

For displacement piles, stress ratio, c_u/σ'_{vo} is correlated with α. Pile slenderness may also be included to modify α with a coefficient F, refer to Equation 2.2 and Figure 2.1 (Tomlinson & Woodward, 2008). During pile driving, the soil surrounding the pile is deformed, experiences excess pore pressure and has low shear strength. The α-factor

is therefore derived using the shear strength of the soil after reconsolidation (when it has regained some of its original strength).

$$f_s = F.\alpha.c_u.A_s \qquad (2.2)$$

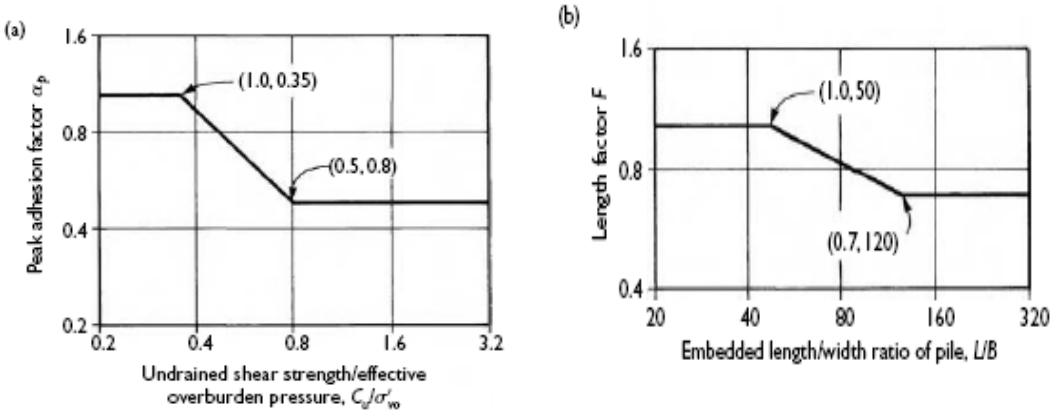

Figure 2.1: Adhesion factors for piles driven deep into clays. (a) Peak adhesion vs C_u/σ'_{vo} (b) Length factor (Tomlinson & Woodward, 2008)

In bored piles, α is related with c_u (Knappett & Craig, 2012):

$\alpha = 1$ for $c_u \leq 30$;

$\alpha = 1.16 - \frac{c_u}{185}$ for $30 \leq c_u \leq 150$; and

$\alpha = 0.35$ for $c_u \geq 150$.

An α-factor of 0.7 is recommended for designing for negative skin friction on piles in Sweden, see Equation 2.3. It is assumed that negative skin friction is active on the pile length where the soil settles more than 5 mm relative to the pile.

$f_s = 0.7\ c_u$ (long term case) (2.3)

Corrected c_u is recommended for undrained case ($\tau_v$from vane test is corrected using liquid limit,w_l; see Equation 2.4). The relation is applicable to normally and slightly overconsolidated clays (Erikson et al., 2004).

$$\tau_{fu} = \mu.\tau_v \qquad (2.4)$$

where $\mu = \left(\frac{0.43}{w_l}\right)^{0.45}$

2.2.2 The β-method

The β-method is an analytical method recommended for cohesionless soils according to Equation 2.5 and 2.6.

$$f_s = \beta . q \quad (2.5)$$

where in cohesionless soil:

$$\beta = K.tan\delta \quad (2.6)$$

and K is the coefficient of lateral earth pressure. K is approximately equal to coefficient of lateral earth pressure at rest (K_0) in bored piles and piles driven into loose sand. In piles driven into dense sands, K may be higher than $4K_0$ (Kezdi & Rethati, 1988)

For over-consolidated clay, β may be determined using an empirical correlation shown in Equation 2.7:

$$\beta = \beta_{NC} . OCR^{0.5} \quad (2.7)$$

β_{NC} is estimated from vane shear data by Equation 2.8:

$$\beta_{NC} = \mu \, (c_u/\sigma'_{vo})_{NC} \quad (2.8)$$

where σ'_{vo} is the effective overburden pressure, OCR is the over consolidation ratio and μ is Bjerrum's correction factor.

The β value may also be correlated with stress ratio through Equation 2.9 (Knappett & Craig, 2012):

$$\beta = 0.52 \frac{c_u}{\sigma'_{vo}} + 0.11 \quad (2.9)$$

A β value of 0.2 is recommended for piles in Sweden where higher values may be used for long term predictions in clay (the recommended range of β is 0.25-0.30) (Erikson et al., 2004)

2.2.3 The λ-method

The λ-method stated in Equation 2.10 has been applied to determine pile skin friction in overconsolidated clays. It has been developed from pile load tests and it is used mainly in marine installations (Bowles, 1997).

$$f_s = \lambda(q' + 2c_u) \quad (2.10)$$

where c_u is the undrained shear strength of the soil, q' is the mid-height vertical effective stress of a soil layer and λ is a coefficient obtained from regression analysis from a large number of pile tests.

2.2.4 Geotechnical end bearing capacity

The bearing capacity of a pile foundation has to be determined in order to estimate the distribution of axial loads when using α and β methods.

In undrained soil situation, the end bearing capacity of a pile is determined using a modified equation for bearing capacity of shallow foundation and is defined in Equation 2.11 (Knappett & Craig, 2012):

$$Q_{bu} = A_P(N_c.C_u) \qquad (2.11)$$

where

A_p = pile cross sectional area

N_c = bearing capacity factor and

C_u = undrained shear strength

In drained soil situation, the end bearing capacity is determined according to Equation 2.12 (Knappett & Craig, 2012).

$$Q_{bu} = A_P(N_q.\sigma'_q) \qquad (2.12)$$

A_p = pile cross sectional area

N_q = bearing capacity factor

σ'_q = overburden pressure

2.2.5 In situ tests

Common in situ tests for estimating skin friction are CPT, static and dynamic load tests.

2.2.5.1 CPT method

Two procedures exist for obtaining axial pile capacities from CPT data; direct and indirect methods. Indirect approach involves first analysing the CPT data to obtain soil properties such as preconsolidation pressure, undrained shear strength and coefficient of earth pressure. Consequently, the soil parameters obtained are used with the relevant analytical or empirical method (e.g. α or β methods) to estimate the pile capacity.

The direct approach estimates the shaft and toe resistance by modifying or scaling CPT measurements (cone resistance - q_c and sleeve friction - f_s). Piezocone CPT can measure pore water pressure in addition to cone and sleeve friction hence corrections for the pore pressures acting on the cone shoulder can be made. Direct CPT methods are well suited for displacement piles as the CPT cone is driven into the soil in a manner that is similar to pile driving (Knappett & Craig, 2012). Due to sensitivity of cone resistance to changes in soil density, it is preferred in some empirical correlations to obtain shaft friction from cone resistance (q_c) instead of sleeve friction (q_s).

The CPT method has the advantage of logging continuous soil strength data; however it may have problems with reliability and difficulties in certain soil conditions. There are large number of CPT correlation methods as described by Fellenius (2014) and (Niazi & Mayne, 2013)

2.2.5.2 Static load tests

Static pile load tests may be used in situations where rare piling conditions are present such as unique pile types, pile installation technique and site conditions (see Figure 2.2). Static load tests may be done in compression and tension to give separate pile shaft and toe capacities. Compressive tests can be done through constant rate of penetration until pile failure or under maintained load where the load is increased in stages while recording settlements and time until 1.5 or 2 times the working load. Loading may also be done to failure. Maintained load test also provide a means for evaluating shaft and toe loads designed by analytical, empirical or numerical methods.

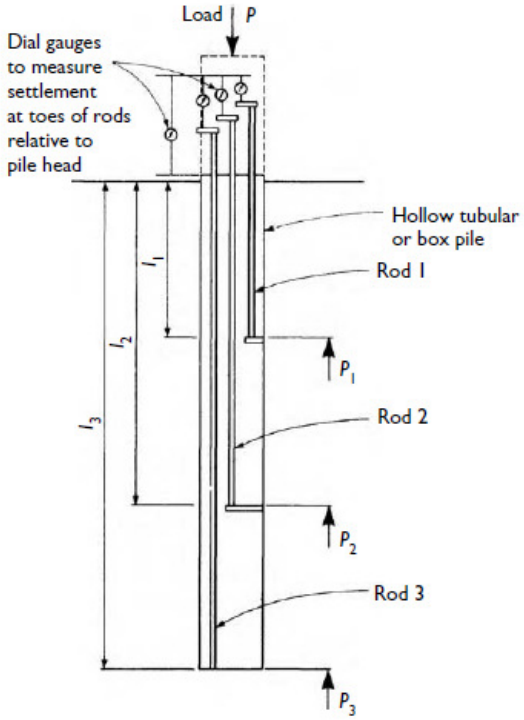

Figure 2.2: Measurement of load transfer from pile to soil at various depths of a pile (Tomlinson & Woodward, 2008)

2.2.5.3 Dynamic load tests

In dynamic load testing, waves are generated by hammer blows and reflected at the pile shaft and toe. These waves are analysed to give shaft and toe resistance. The

method is able to separate pile and shaft resistance and it can also be used in integrity testing of piles.

2.3 Numerical methods

Simplified methods of analysis such as the empirical methods discussed in Chapter 2.2 overestimate the mobilized skin friction (Lee et al., 2002). Numerical modelling methods for example the load transfer method and the finite elements (FEM) may be used to give more optimized estimations.

2.3.1 Load transfer method

The load transfer method uses load transfer curves or functions that relate interface shear or toe resistance with pile displacement at discretized sections of the pile. Analysis involves assumption of a displacement at the pile toe and then using the load verses displacement curves to determine the axial loads for each discretized pile section from the toe to the pile head. If the displacement at the pile toe does not result in a correct applied axial load at the pile head, the procedure is iterated.

Load transfer functions consist of t-z, q-z and p-y curves which represent shaft, toe and lateral stiffness respectively. These curves are obtained from observations of load deformation behaviour in instrumented piles (see Figure 2.3). To model a pile with load transfer method, a number of curves are required for each soil layer and type of pile. There are limitations with the load transfer method for example in the way the deformations at different levels of the pile are treated independently and difficulties in extrapolating the analysis e.g. due to changes in soil conditions adjacent to the pile.

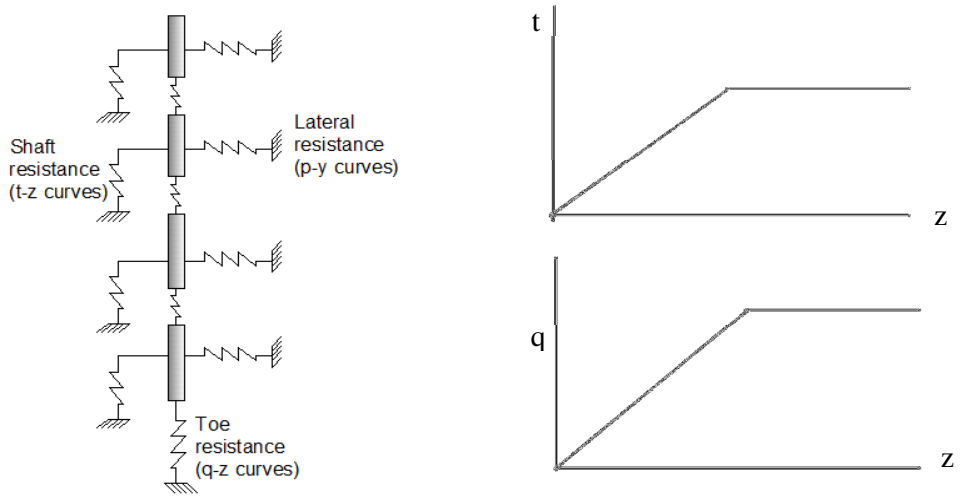

Figure 2.3: Discretised pile model and typical load displacement curves (Modified from (Bowles, 1997))

2.3.2 Finite elements method (FEM)

FEM is an advancement over load transfer method. It allows intrinsic properties of soils to be applied in the models. The division of soil-structure into elements makes it easier to model more complicated problems such as complex soil layering, geometry and consolidation. One setback of FEM is the large data and computational power needed. FEM is discussed further in the following section.

2.4 Finite elements analysis and PLAXIS

FEM involves discretization of a boundary value problem into a series of interconnected finite elements. These elements could be 1-D, 2-D or 3-D. Element equations are developed in form of shape and interpolating functions. A global stiffness matrix is assembled and solved so as to satisfy known boundary conditions (see Equation 2.13).

$$[K]\{U\} = \{P\} \qquad (2.13)$$

where $[K]$ is the stiffness matrix, $\{U\}$ are nodal displacements, $\{P\}$ are nodal loads whereas the relationship between $\{U\}$ and $\{P\}$ is a known constitutive law.

In this analysis, PLAXIS FEM software has been considered for analysis. PLAXIS is a commercial finite element software for solving geotechnical engineering problems such as deformation, stability and groundwater flow. It has been chosen due to its wide use in geotechnical engineering and its implementation of advanced soil models. The Soft Soil model in PLAXIS anniversary edition version 2.0 is used to model the soil as it is recommended for compressible soils.

In order to perform full numerical analysis of a pile foundation, constitutive models for the pile, soil and pile-soil interface are required. These are described in the following sections

2.4.1 Linear elastic model

In linear elastic models, a material is characterised by elastic properties such as shear modulus, G and bulk modulus, K. Linear elastic models are often used to model structural parts of the model for example steel or concrete elements.

2.4.2 Interface constitutive model

Pile-soil interaction is modelled using interface elements. These interface elements allow relative displacement in terms of slipping and gapping. A linear elastic, perfectly plastic constitutive relationship is commonly implemented in FEM for the interface. The interface model follows a Mohr-Coulomb law where Equation 2.14 is a failure line and Equation 2.15 refers to plastic potential (Boulon et al., 1995):

$$f = \tau - \sigma_n . tan\delta \qquad (2.14)$$

$$g = \tau - \sigma_n . tan\psi \qquad (2.15)$$

The strength parameters for the interface are obtained from a direct shear test where the pile material is sheared against the soil in shear box equipment (Knappett & Craig, 2012).

2.4.3 Constitutive soil model

Advanced critical state soil models use elastoplastic laws to predict soil behaviour. Deformations can be calculated due to stresses and vice versa through Equation 2.16 (Potts, 1999):

$$[\Delta\sigma] = [D^{ep}] [\Delta\varepsilon] \qquad (2.16)$$

where $[D^{ep}]$ is an elastoplastic stiffness matrix.

Total strains are divided into elastic and plastic strain, see Equation 2.17.

$$[\Delta\varepsilon] = [\Delta\varepsilon^e] + [\Delta\varepsilon^p] \qquad (2.17)$$

Incremental stress during elastic state is proportional to incremental strain, see equation 2.18.

$$[\Delta\sigma] = [D] [\Delta\varepsilon^e] \qquad (2.18)$$

where $[D]$ is an elastic stiffness matrix.

Incremental plastic strains, $\Delta\varepsilon^p$ are related to the plastic potential through a flow rule which determines the direction and magnitude of plastic strains. A yield function is defined that separates elastic and plastic behaviour. A hardening or softening rule is

also included to differentiate the response of normally consolidated and highly consolidated soils to shear deformation. In the following section, the Soft Soil model is introduced.

2.4.3.1 Soft Soil model (SSM)

SSM is based on Cam-clay and is suited for nearly-normally consolidated clay, clay silt and peat soils which are highly compressible. The main features of SSM that is implemented in PLAXIS are briefly described.

In SSM, volumetric strains are logarithmically related to the mean effective stresses, so that under virgin compression and unloading-reloading it is expressed as (refer to Figure 2.4, Equation 2.19 and Equation 2.20):

$$\varepsilon_v - \varepsilon_v^0 = -\lambda^*.ln\left(\frac{p\prime}{p^0}\right) \qquad (2.19)$$

$$\varepsilon_v - \varepsilon_v^0 = -\kappa^*.ln\left(\frac{p\prime}{p^0}\right) \qquad (2.20)$$

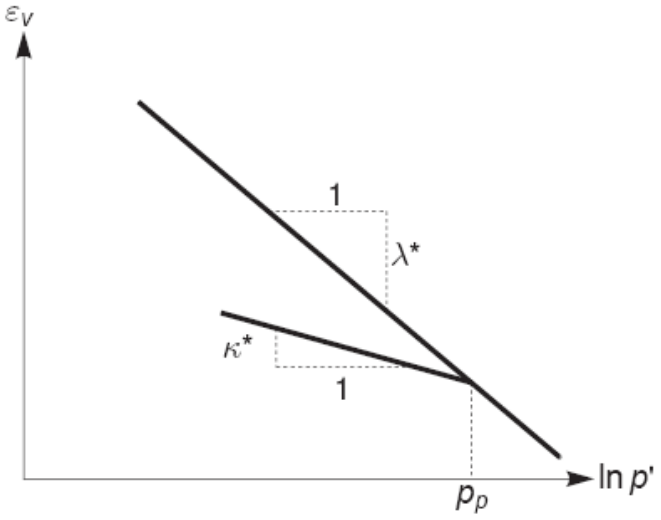

Figure 2.4: Volumetric strain-mean stress relationships in Soft Soil model (Brinkgreve et al., 2014)

The yield function in SSM is an ellipse where parameter M determines the height of the ellipse while P_p determines its width (see Figure 2.5). The soil state on the yield surface undergoes irreversible volumetric strain deformations as the yield surface expands which is described by movement along the primary compression line. Inside the yield curve, the soil experiences reversible deformations described by the swelling lines. The yield curve is given as by Equation 2.21:

$$f_c = \frac{q^2}{M^2} + p'(p' - p_c) \qquad (2.21)$$

The Mohr Coulomb failure surface is defined by Equation 2.22:

$$f_f = \frac{1}{2}(\sigma'_1 - \sigma'_3) + \frac{1}{2}(\sigma_1 + \sigma_3)\sin\phi' - c.\cos\phi' \qquad (2.22)$$

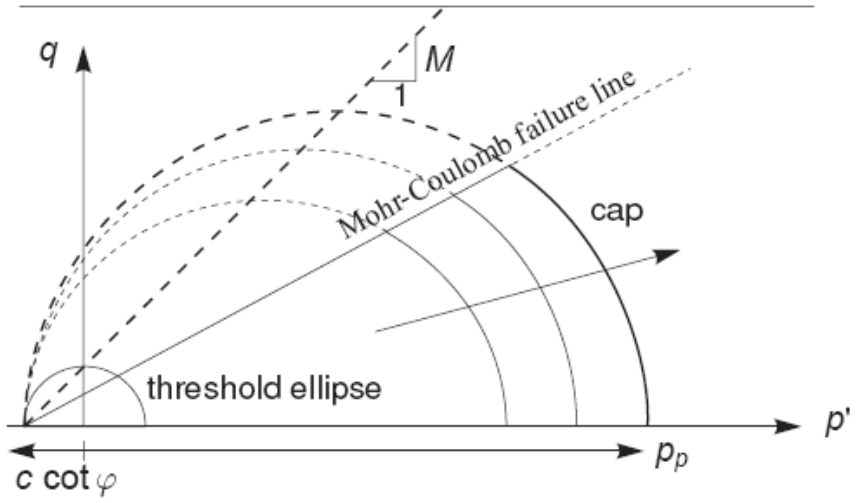

Figure 2.5: Yield surface for SSM projected into p'-q plane (Brinkgreve et al., 2014)

The main input parameters for SSM are initial state parameters (K_0, OCR or POP), compression parameters (λ^*, κ^* and v_{ur}), and strength parameters (ϕ', c' and ψ). These parameters are obtained from isotropic triaxial tests. The compression parameters can also be derived from one dimensional consolidation (oedometer) test, i.e. from C_c and C_s as shown in equation 2.23 to 2.24 and from Cam-clay parameters as shown in equations 2.25 to 2.26.

$$\lambda^* = \frac{C_c}{2.3(1+e_0)} \qquad (2.23)$$

$$\kappa^* \approx \frac{2C_s}{2.3(1+e_0)} \qquad (2.24)$$

$$\lambda^* = \frac{\lambda}{(1+e)} \qquad (2.25)$$

$$\kappa^* = \frac{\kappa}{(1+e)} \qquad (2.26)$$

There are also correlations to obtain the compression parameters from the Swedish CRS test results for example in Olsson (2010) or from plasticity indices (Brinkgreve et al., 2014)

3 METHODOLOGY

The initial stage involves an evaluation of the PLAXIS 2D software to predict stresses at a soil structure interface. Thereafter, a model pile test is developed in prototype scale to analyse a centrifuge pile test in order to evaluate the numerical model and the method of analysis.

3.1 Modelling a pile in PLAXIS 2D

There are currently four methods of modelling a pile in PLAXIS 2D: Plate element, node to node anchor, embedded pile row and volume elements. Embedded pile elements allow for interaction between pile and soil with a continuous mesh between pile rows therefore it can model better the effects of both axial and lateral loads (Brinkgreve, 2014). In embedded pile rows, ultimate skin resistance and bearing capacity are input parameters (it is not output of numerical analysis). It does not allow input of interface properties for example the interface friction angle and the interface stiffness parameters have to be calibrated.

Node to node anchors do not allow for pile-soil interaction and it does not allow input of pile bending stiffness. This makes it difficult to model lateral loads. The foot consists of a node and this may lead to mesh dependent results (Brinkgreve, 2014).

Plate element elements when used with an interface is a good choice when modelling sheet piles in plane strain mode but is not the best method to model a pile. This is because plate elements in 2D are continuous in the out of plane direction hence only pile-soil interaction occurs. This makes it difficult to obtain the correct load and deformation of a pile (Brinkgreve, 2014).

In using volume elements, the soil is replaced with pile material and an interface is provided between the pile and soil. This method has been adopted because it gives the possibility to model a single pile in axisymmetric condition. Plate elements may be included in the pile volume to give output of pile axial loads and bending moments. However, this method cannot be used to analyse piles with non-circular cross section and pile groups.

3.1.1 PLAXIS soil structure interface

The interface is the point of contact between the pile and adjacent soil, where skin friction is mobilized. It is therefore important to understand its behaviour in PLAXIS in order to properly predict stresses at the pile-soil interface.

R_{int} is a parameter varying between 0.01 and 1 for adjusting the interface strength relative to that of adjacent soil. Its role is illustrated in equations 3.1 to 3.2.

The interface in elastic state is given by Equation 3.1.

$$|\tau| < -\sigma_n . tan\varphi_{int} + c_{int} \qquad (3.1)$$

Interface in plastic state is given by Equation 3.2.

$$|\tau| = -\sigma_n . tan\varphi_{int} + c_{int} \quad (3.2)$$

where $c_{int} = R_{int}.c_{soil}$ and $tan\phi_{int} = R_{int}. tan\phi_{soil}$

The stiffness at the interface is also reduced according to Equation 3.3.

$$G_i = R^2{}_{int}. G_{soil} \leq G_{soil} \quad (3.3)$$

The interface is modelled after an elastic-perfectly plastic constitutive law where during elastic state small, recoverable displacements occur, while permanent displacements occur in plastic state. When a more advanced model is set for the interface or surrounding soil, only the basic parameters for Mohr coulomb C, ϕ, ψ, E and ν are accepted (Plaxis, 2013). The interface elements consist of node pairs in soil and structure, which interact with two elastic-perfectly plastic springs. One spring models gap while the other models slip displacement. Slipping and gapping at the interface is described with Equations 3.4 and 3.5.

$$Elastic\ gap\ displacement\ = \frac{\sigma}{K_N} = \frac{\sigma.\ t_i}{Eoed_i} \quad (3.4)$$

$$Elastic\ slip\ displacement\ = \frac{\tau}{K_S} = \frac{\tau.\ t_i}{G_i} \quad (3.5)$$

where G_i is the shear modulus, $Eoed_i$ is one dimensional compression modulus, t_i is virtual thickness of the interface, K_N is the elastic normal stiffness and K_S is elastic interface stiffness.

An elastoplastic interface element shown in Figure 3.1 is implemented in PLAXIS and consists of triangular 6 nodded or 15 nodded elements sharing node pairs at the interface of two materials.

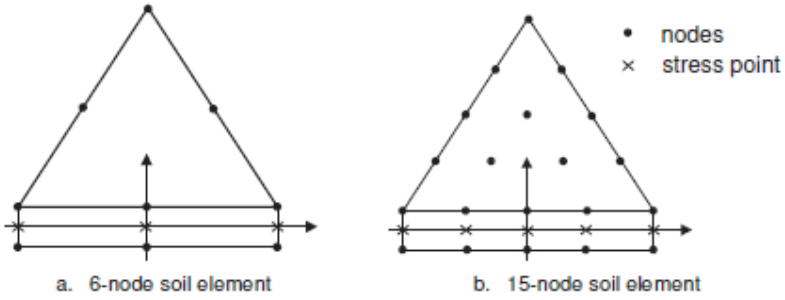

Figure 3.1: Nodes (dots) and integration points (crosses) at an interface (Brinkgreve et al., 2014)

An investigation is done to understand the behaviour of PLAXIS interface. Both plastic and consolidation analysis was carried out as described below:

i) Plastic analysis

A simple model was set up in order to predict the average shear stress at an interface. It consists of a 2-D elastic concrete block 4 m long by 1 m high that is sheared on an interface by applying a prescribed displacement of 10 mm. The properties of the interface and the block are summarised in Table 7.1 of appendix A1. The results of plastic analysis are presented thereafter in Appendix A1. From the analysis, full shear resistance was mobilized thus the shear stress was a maximum for each normal load applied.

The results indicate that the interface shear stress increases or decreases proportionately with interface strength reduction factor R_{int}. The predicted interface shear with R_{int} of unity differed by 0.01 kN/m^2 with the average shear estimated using Mohr-Coulomb theory ($\tau_{max} = R_{int}.c' + \sigma'_n.R_{int}.tan(\phi')$.

ii) A comparison between drained plastic analysis and long term consolidation analysis

The material properties listed in Table 7.1 of appendix A1 were applied where in this case a small section (1 m x 1 m) of a pile-soil is investigated (see Figure 7.6 of appendix A2). Both drained plastic analysis and long term consolidation analysis was carried out. The interface properties are set to be the same as those of the adjacent soil by using R_{int} of unity. The soil was sheared against a static elastic block with an interface in between the two materials by prescribing a vertical displacement of 100 mm and a lateral displacement of 10 mm from the right. Consolidation analysis was carried out for 500 days for the excess pore water pressure fully dissipate.

The results indicate negligible differences in shear and effective stresses obtained from drained plastic and consolidation analysis. There is little influence of pore water on shear stress in conditions where normal loads are similar (See Figure 7.7 of appendix A2).

This illustrates that long term behaviour can be studied with simple drained plastic analysis while still giving similar result as long term consolidation analysis.

3.2 Case study: A centrifuge model pile test

This section focusses on a case study of a documented centrifuge pile test where negative skin friction is triggered by lowering of the water table. The test was described in detail by Lee et al., (1998) and Lee & Chen, (2003). It was carried out to investigate down drag caused by excessive groundwater withdrawal. First, a general description of a centrifuge test is given in the following chapter and thereafter the numerical model developed in PLAXIS is described.

3.2.1 Laboratory centrifuge test

In order to evaluate a numerical model and a method of analysis, it is valuable to compare the output of a model with results from an instrumented pile in the field or a laboratory test. In this study, a scaled down laboratory pile test has been chosen for this purpose.

Centrifuge tests are preferred to full scale tests on piles due to cost, time and level of control they allow during testing. According to Tomlinson & Woodward (2008), scaled down models may be used as a general research tool as long as their results can replicate pile installation method and the results verified by full-scale tests. Some of the uses of centrifugal modelling are prototype modelling, investigation of geotechnical problems, parametric studies and validation of numerical methods (Ng, 2013). Full scale testing, centrifuge modelling and numerical modelling complement each other and none of these approaches is perfect for every geotechnical problem (see Figure 3.2).

Figure 3.2: Relationship between centrifuge modelling, numerical modelling and full scale field testing (Ng, 2013)

The principle behind centrifuge modelling is recreating stress level and gradient in real world piles by increasing the gravitational acceleration n times in a 1/n scale model, where $n = r.\omega^2/g$ (where r is the arm radius, ω is angular velocity and g is gravitational acceleration). The increased stress is generated by centripetal acceleration as the model revolves. In Figure 3.3 for example, the sketch illustrates an embankment model in a centrifuge.

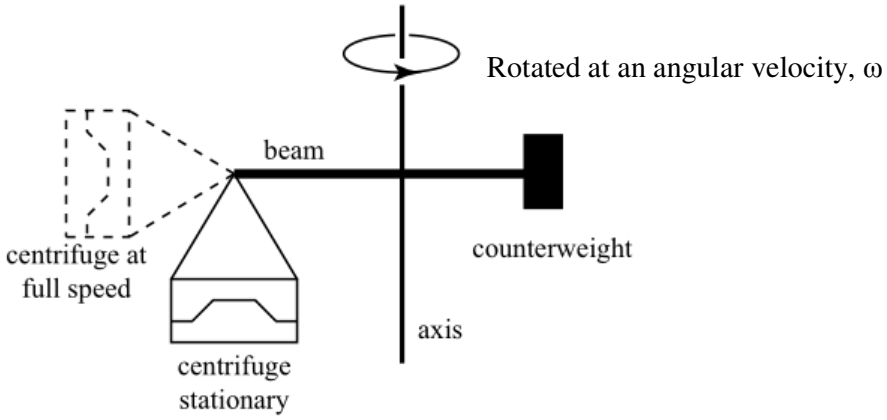

Figure 3.3: Diagram of a beam centrifuge swinging (Muir Wood, 2004)

Other benefits of a scaled down models include shorter drainage paths which reduce time of consolidation by a factor $1/n^2$ (Ng, 2013). Laws governing the relationship between model and prototype are derived using dimensional analysis or from similarity between prototype and model (Table 3.1 shows some of the factors for scaling parameters between model and prototype).

Ng (2013) also suggests that prior to calibrating constitutive models and model parameters against historical cases; it is a good practice to use physical models to provide known boundary and ground conditions. This minimizes uncertainties in material, ground, and boundary conditions during calibration.

Table 3.1: Factors for scaling centrifuge tests, modified from (Ng, 2013)

Parameter	**Scaling factor (model/prototype)**
Acceleration	*n*
Linear dimension	*1/n*
Stress	*1*
Strain	*1*
Mass	$1/n^3$
Density	*1*
Unit weight	*n*
Force	$1/n^2$
Permeability	*n*
Displacement	*1/n*
Time (consolidation)	$1/n^2$
Time (creep)	*1*

Site investigations in centrifuge tests are normally done by adopting scaled down versions of prototype techniques such as the CPT, piezometers and shear vane tests. Once the desired acceleration has been achieved, installed instrumentation is used to record physical processes such as displacements, stresses and bending moments.

There are some limitations encountered in centrifuge modelling. One of these is effects from soil grain size that occur if structural elements are scaled to a smaller size while the soil particles sizes remain constant. This difference is usually minimized by using smaller average soil grain size or by increasing model pile diameter. The scaling of the shear zone adjacent to the pile (assumed to be 10% of pile diameter) differs for different pile sizes. This affects the shear stress at the interface where the effect is greater in small model piles. It is suggested that the ratio of the pile diameter to mean grain size (d_{50}) should exceed 35 and 44 for vertical and horizontal pile loads respectively (Lundberg et al., 2012). It is also difficult to recreate similar soil conditions as those in the field through soil reconsolidation. Moreover, there exists a non-uniformity of the gravity field which increases in proportional with soil depth though this problem can be resolved by using a centrifuge with a longer arm.

3.2.2 Soil and pile properties

The tested soil specimen was silty clay with a plasticity index of 5 and an effective grain size (D_{10}) of 0.003 mm. One dimensional consolidation and direct shear tests were carried out on the soil which resulted in the following properties:

Table 3.2: Silty clay soil (soft soil material) and interface properties, from (Lee et al., 1998)

Depth (m)	**e_o**	**γ_{dry} (kN/m³)**	**γ_{sat} (kN/m³)**	**C_c**	**C_s**	**POP (kPa)**	**Φ (°)**	**δ (°)**	**Su/ σ_v'**	**k (m/d)**	**ν_{ur}**
22.5	1.4	11	17	0.15	0.036	117	32	25.8	0.32	0.00864	0.12

The oedometric parameters C_c and Cs were converted to Soft Soil model parameters λ^* and κ^* using the Equations 3.6 and 3.7. It is also possible to directly input C_c and C_s in Soft Soil model.

$$\lambda^* = \frac{C_c}{2.3(1+e_0)} = 0.0272 \qquad (3.6)$$

$$\kappa^* \approx \frac{2C_s}{2.3(1+e_0)} = 0.0130 \qquad (3.7)$$

The saturated density and void ratio of the soil at the start of the test was estimated from the effective overburden pressure where it is assumed that the specific gravity of the soil is 2.65. This gave a saturated density of 17 kN/m^3 and a void ratio of 1.4,

which are assumed to be uniform throughout the soil depth (see Table 7.2 of appendix A2). The hydraulic conductivity of 0.00864 m/d was obtained from Lee & Chen (2003) and was assumed to be similar in vertical and horizontal directions. The lower boundary below the clay consisted of a 2.5 m thick drainage sand layer whose properties were not specified.

Though the pile material is steel, the pile was fabricated so that after scaling it behaved like a concrete pile. The properties of the "concrete pile" are listed in Table 3.3.

Table 3.3: Pile properties (Linear elastic material)

Diameter (m)	**Length (m)**	**E(kPa)**	**ɣ (kN/m^3)**	**ν**
1.5	22.5	50e^6	24	0.3

3.2.3 Test setup

A drainage layer of sand with a thickness of 2.5 m (prototype scale) was put at the bottom of the consolidometer before the remoulded silty-clay slurry was poured in. The soil was consolidated to the required maximum preconsolidation pressure of 117 kPa.

The model pile was installed using a guiding tube into the prepared soil bed as shown in Figure 3.4 and then it was put into the centrifuge for acceleration.

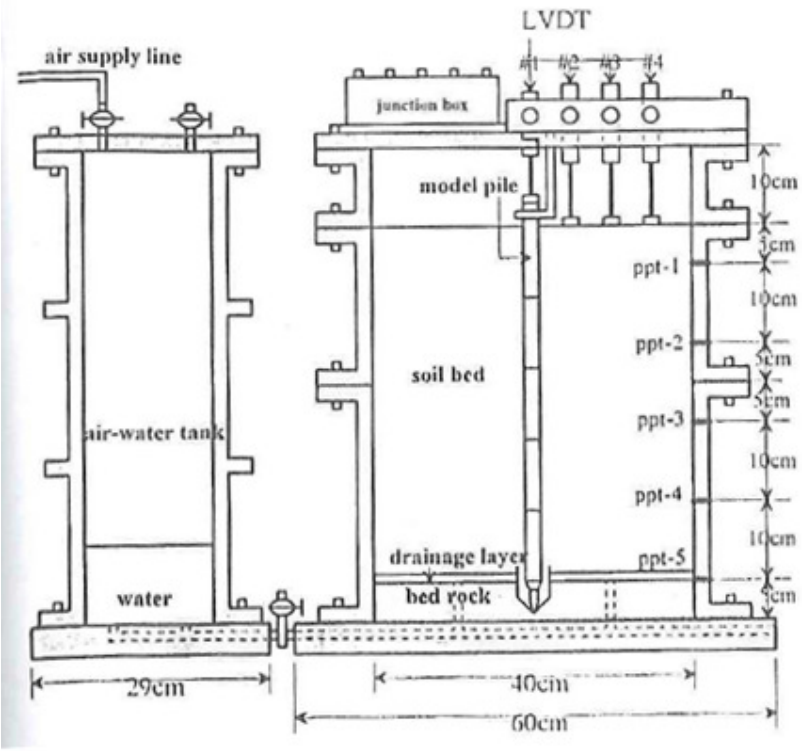

Figure 3.4: Setup of the test (Lee et al., 1998)

The test was carried out in several stages and only the important stages that will be modelled are mentioned. The model was accelerated to 50-g while maintaining the water level at the ground surface. The excess pore water pressures were let to fully dissipate through self-weight consolidation. Once equilibrium conditions were achieved,

1. The water level was lowered from the initial level at ground surface by 6 m within 15 ± 5 days.
2. Then soil was let to consolidate under its own weight for about 162 ± 10 days for excess pore water to dissipate. Total consolidation period is therefore 177 days in prototype scale (equivalent to 102 minutes in model scale)

3.2.4 Numerical model in PLAXIS

The installation of the pile was done at normal gravity conditions (1g) hence it is assumed to be a bored pile where the effects of installation can be ignored. The pile model is therefore created by replacing soil material with pile material.

i) Model geometry

A two dimensional axisymmetric model was developed in the commercially available software code PLAXIS. The radius and depth of the model was set to 40 m by 22.5 m respectively (refer to Figure 3.5). The boundary conditions were set as follows: the

left and right boundaries were fixed horizontally and free in vertical direction, the bottom boundary is fixed in both directions while the top boundary is free. The symmetry line and the right boundary were closed while the top and bottom boundaries are open to groundwater flow. The initial water level was set at the ground surface.

The mesh consists of 15 nodded triangular elements for the pile and soil. A vertical interface is placed between the pile and soil and another horizontal interface is set at the toe. The mesh of the soil closer to the pile and that of the pile were refined while the rest is left to default (course). The mesh consists of 1763 elements and 14603 nodes.

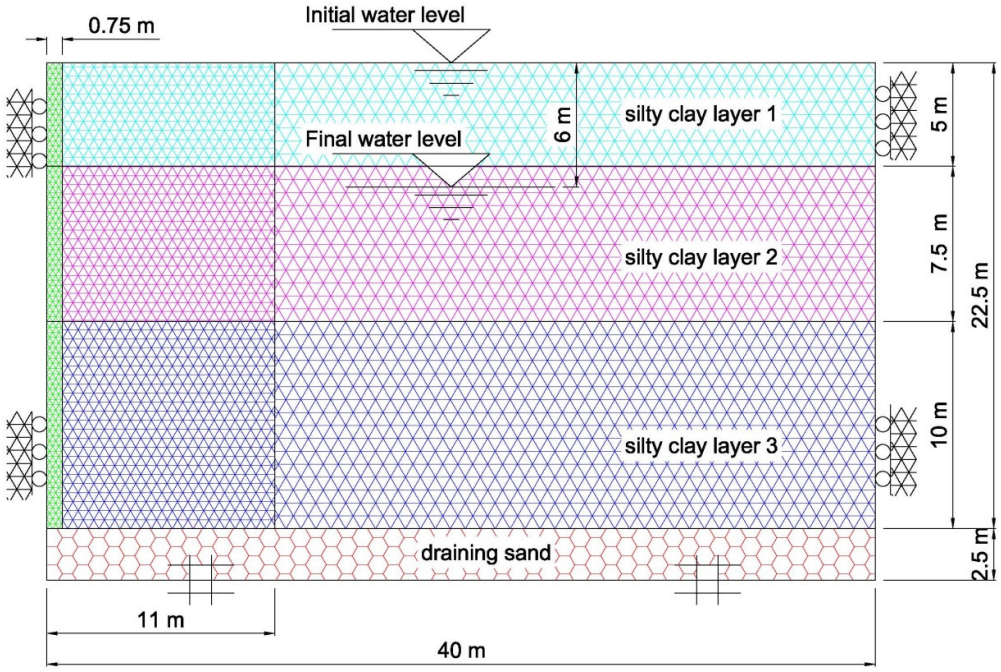

Figure 3.5: Schematic of the model

The silty clay soil was modelled with three layers of thickness of 5, 7.5 and 10 m. Since the tested soil consisted of one homogeneous layer, the subdivision into different layers was motivated by the variation of OCR with depth and hence a non-uniform K_0. The value K_0^{NC} was estimated from the Jaky's formula in Equation 3.8.

$$K_0^{NC} = 1\text{-}\sin(\phi') \quad (3.8)$$

Average K_0 was estimated for each of the layers from the mean OCR so that $K_0 = K_0^{NC}\sqrt{OCR}$. A constant preoverburden pressure (POP) of 117 kPa was applied on each layer. An interface with a strength reduction factor of 0.774 relative to the adjacent soil was implemented (see Equation 3.9).

$$R_{int} = \frac{\tan\delta}{\tan\Phi} = \frac{\tan 25.8}{\tan 32} = 0.774 \quad (3.9)$$

The lower boundary that consists of a drainage sand layer whose properties were not specified in the test is modelled first as an infinitely stiff material and secondly as an elastic material.

ii) Analysis procedure

K_0 procedure was used to initialize the numerical model. This procedure was chosen due to flat ground around the pile which could not pose equilibrium problems during initialization. During K_0 initialization, the coefficient of lateral earth pressure K_0 is used to generate the horizontal stresses, σ'_h from vertical overburden pressure σ'_v where $\sigma'_h = K_0 . \sigma'_v$.

An intermediate plastic calculation step was included in which the pile was introduced into the soil by replacing the soil material with pile material. Then the consolidation stage followed that began by resetting deformations from the plastic calculation.

The water table was lowered gradually from its initial level at the ground surface using a linear function by 6 m over 15 days. Pore pressures were set to be calculated using a coupled calculation. Consolidation took 162 days; hence the simulation runs for duration of 177 days.

4 RESULT

The result of the numerical analysis is presented in the following chapters.

4.1 The base as infinitely stiff

The result for the scenario where the draining sand layer is modelled as an infinitely stiff material is presented in the following sections.

4.1.1 Vertical effective stresses

The profiles of effective stresses presented by Lee et al. (1998) and fit well with result calculated with PLAXIS 10 m away from the pile both before and after lowering of the groundwater table. Closer to the pile (2 m), there is a reduction in effective stresses by 5-10 kN/m^2 below the depth of 6 m which are caused by the loading of the soil on the pile through skin resistance at the interface. The increase in affective stress at each depth corresponds to the weight of the water that is lowered by 6 m (see Figure 4.1).

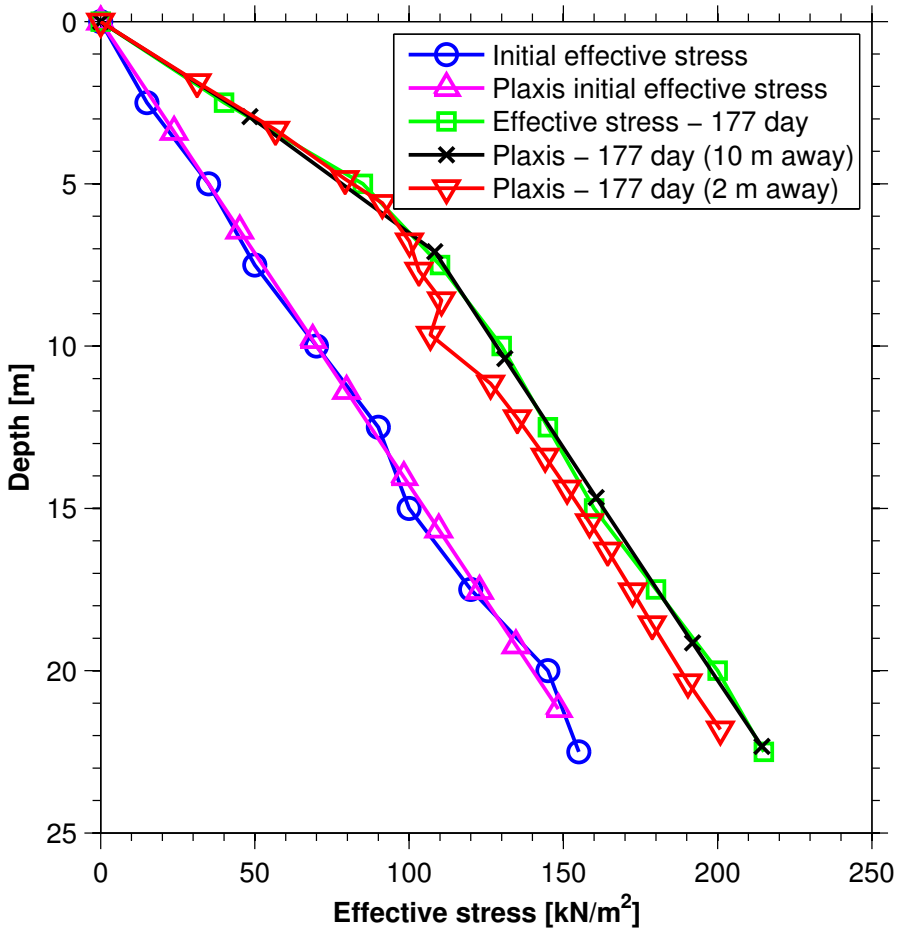

Figure 4.1: Effective stresses before and after lowering the water table

4.1.2 Ground and pile head settlements

The calculated ground settlement in PLAXIS at the end of consolidation was 0.13 m at the end of the test, see Figure 4.1. This is a 35% underestimation when compared with the measured ground settlements of 0.2 m. The measured pile head settlements and that calculated with PLAXIS were 25 and 0.2 mm respectively (simulated result is lower than the measurement by 99%). Since the pile is very stiff relative to the soil, it is possible that the difference between the measured and the settlements calculated from PLAXIS is due to compression or consolidation of the drainage sand layer below the silty clay soil which may have occurred during the test.

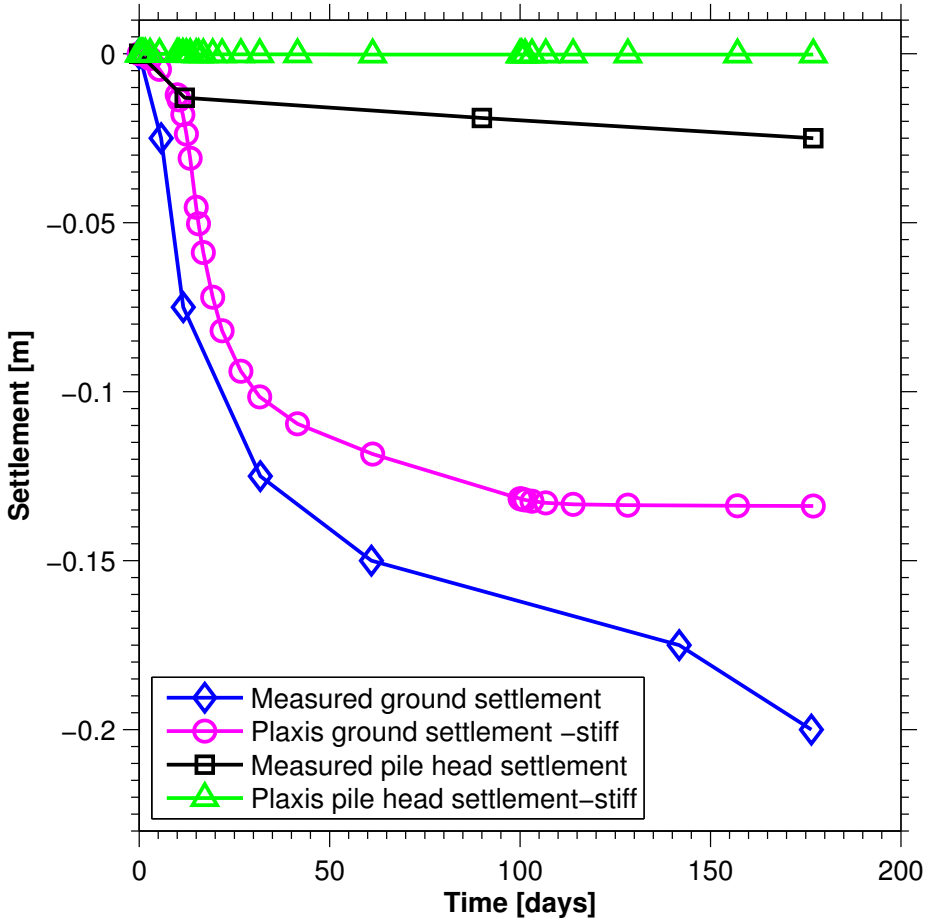

Figure 4.1: Measured and PLAXIS calculated ground settlement at various stages of consolidation

4.1.3 Skin friction

The least shaft friction of less than 2 kPa is mobilized after a day due to small soil settlements (less than 1 mm, in Figure 4.1).

Maximum skin friction is achieved almost immediately after the water table is lowered by 6 m (i.e. after 15 days). Skin friction is over estimated as shown in result calculated with PLAXIS in Figure 4.2.

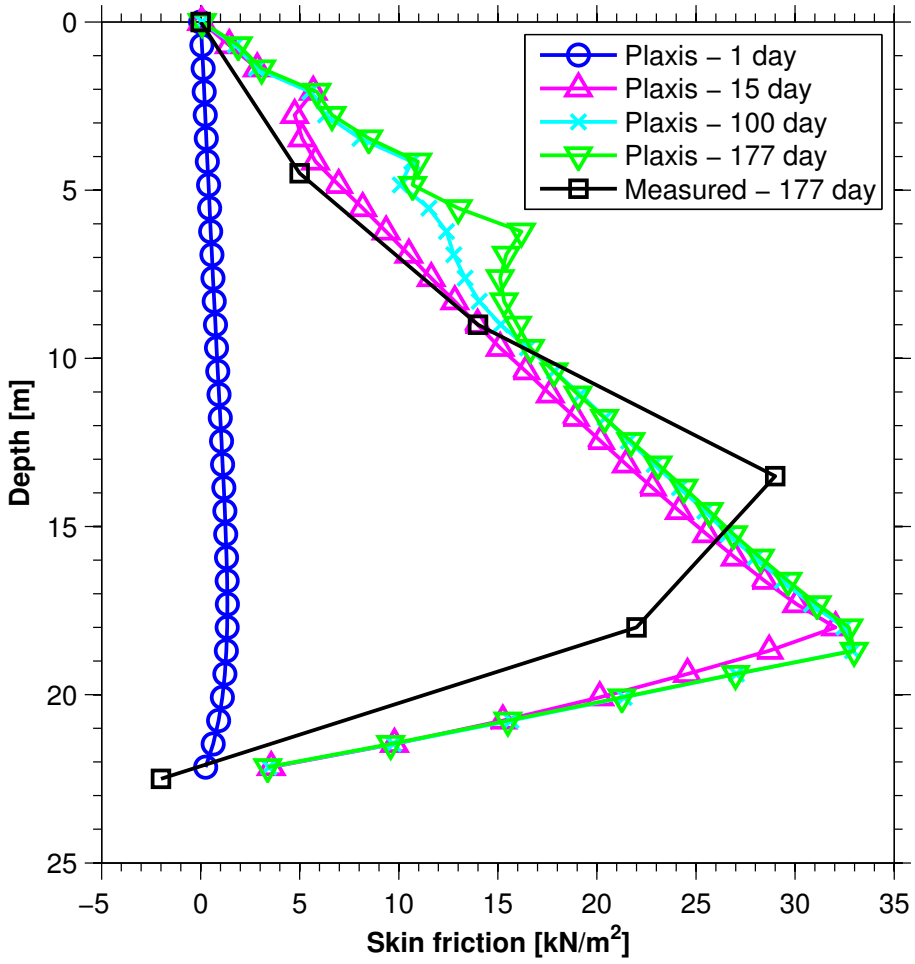

Figure 4.2: Comparison between PLAXIS calculated and measured skin friction

4.1.4 Axial load distribution

The maximum axial loads calculated with PLAXIS exceed the measured value by 80% (see figure 4.3). This is expected because there is difference in measured and calculated pile-soil settlements.

Due to the infinitely stiff base that supports the pile in the model, the neutral plane is located at the pile toe. This is different from the location observed in the measured result that is at a depth of 18 m.

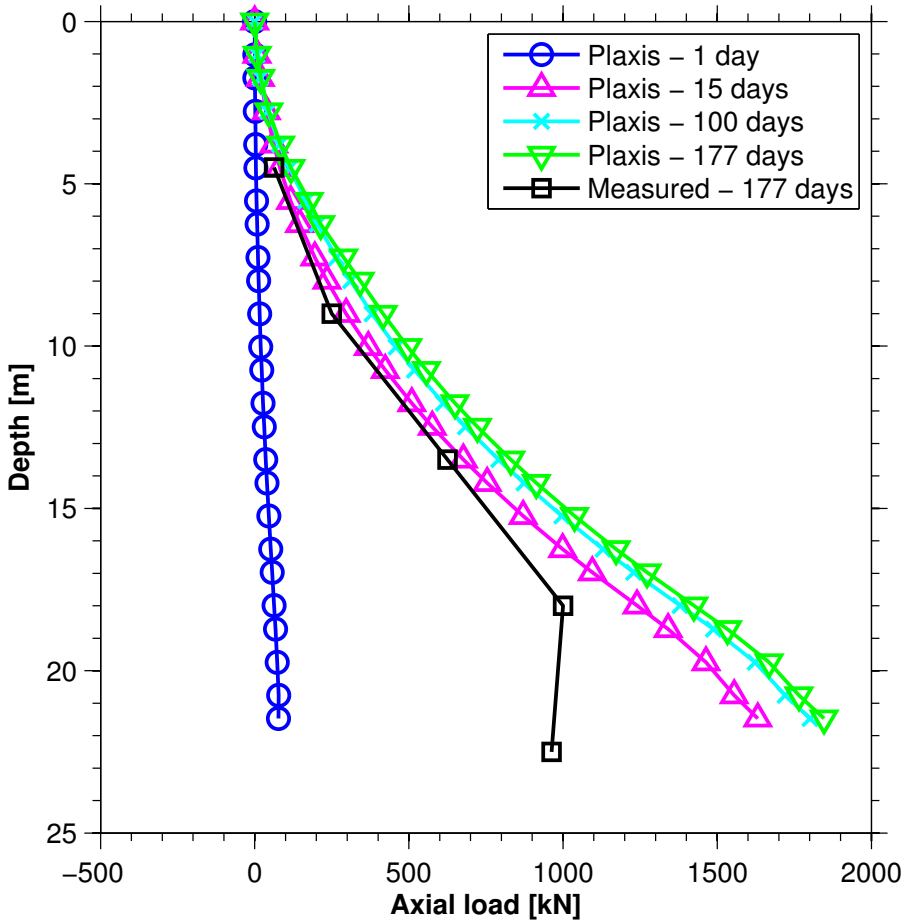

Figure 4.3: Comparison between PLAXIS calculated and measured axial loads

4.2 Modelling with an elastic drainage sand layer

The result for the scenario where the draining sand layer is modelled as an elastic material is presented in the following sections.

4.2.1 Ground and pile head settlements

In the previous result there were differences between measured and calculated pile head settlements and axial loads. This could be related to pile settlement due to the deformation of the sand layer that drains out excess pore water below the clay. An elastic modulus, E of 20,000 kPa is deduced from the difference between measured and calculated value of pile head settlement in Figure 4.1. To simulate this drainage sand layer, a free draining elastic layer of 2.5 m thickness with above estimated E is introduced.

In Figure 4.4, the calculated pile head settlement is closer to the measured result. The ground settlement has also increased marginally by 5 mm. This is less than the pile head settlement, which increased by 20 mm, since the pile carries drag load in addition to its self-weight.

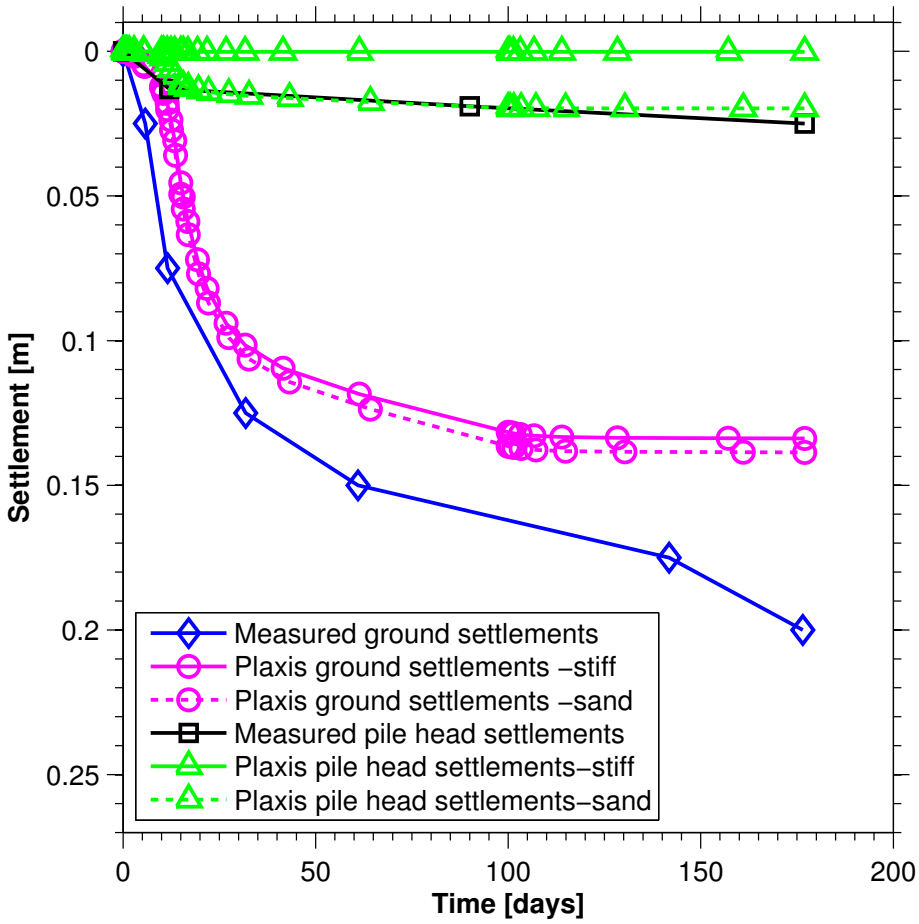

Figure 4.4: PLAXIS calculated settlements compared with measured settlements at ground surface (5 m away from the pile) and at the pile head

4.2.2 Skin friction

A maximum negative skin friction of 28 kPa and positive skin friction of 40 kPa is calculated at the end of consolidation in PLAXIS (see Figure 4.5). Long term skin friction estimated from an α-factor of 0.7 as used in Sweden is slightly higher than the measured as well as the PLAXIS result. The calculation according to Swedish practice assumes that there is no skin friction when relative pile-soil settlements are less than 5 mm.

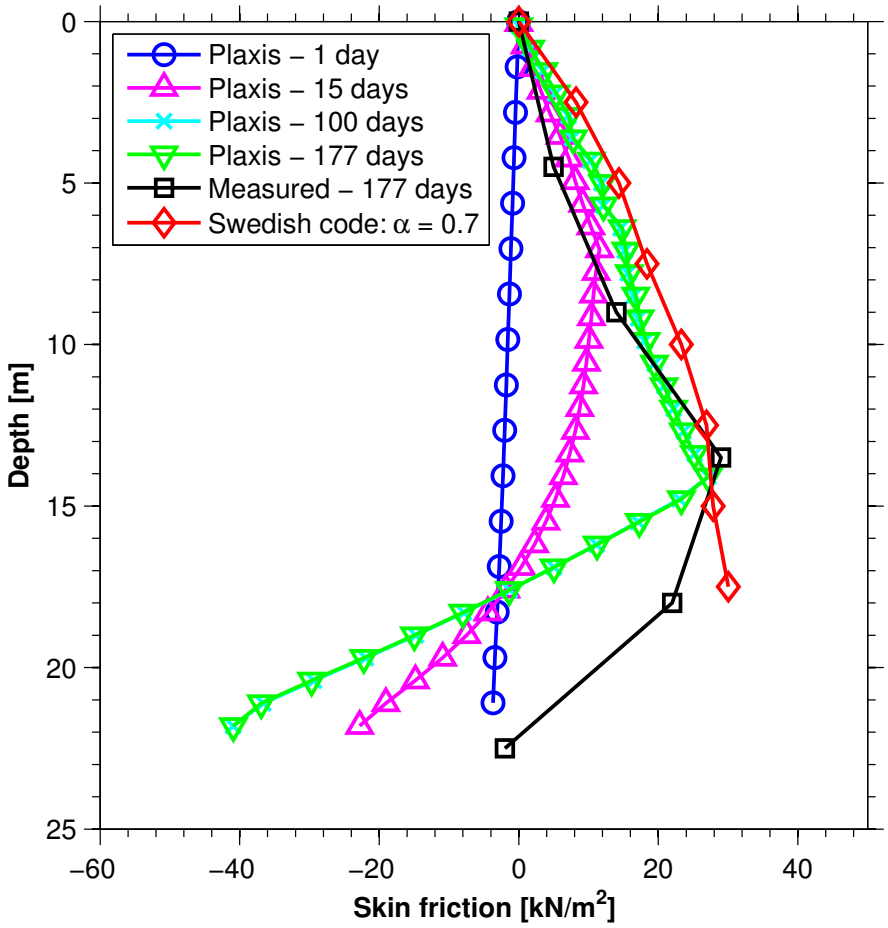

Figure 4.5: Comparison of skin friction calculated from PLAXIS and the α-method according to Swedish practice with the measured skin friction.

4.2.3 Axial load distribution

Initially after one day, there is positive shaft resistance due to the pile settling more than the soil (see Figure 4.6).

The result shows that the calculated axial loads exceed the measured value by 17% at the end of consolidation. The increase in relative pile-soil settlements due to the deformation of the sand layer increases the positive shaft resistance, raises the

location of the neutral plane and decreases the maximum axial forces. An α factor 0.7 gives an axial force 76% higher than that measured from the test.

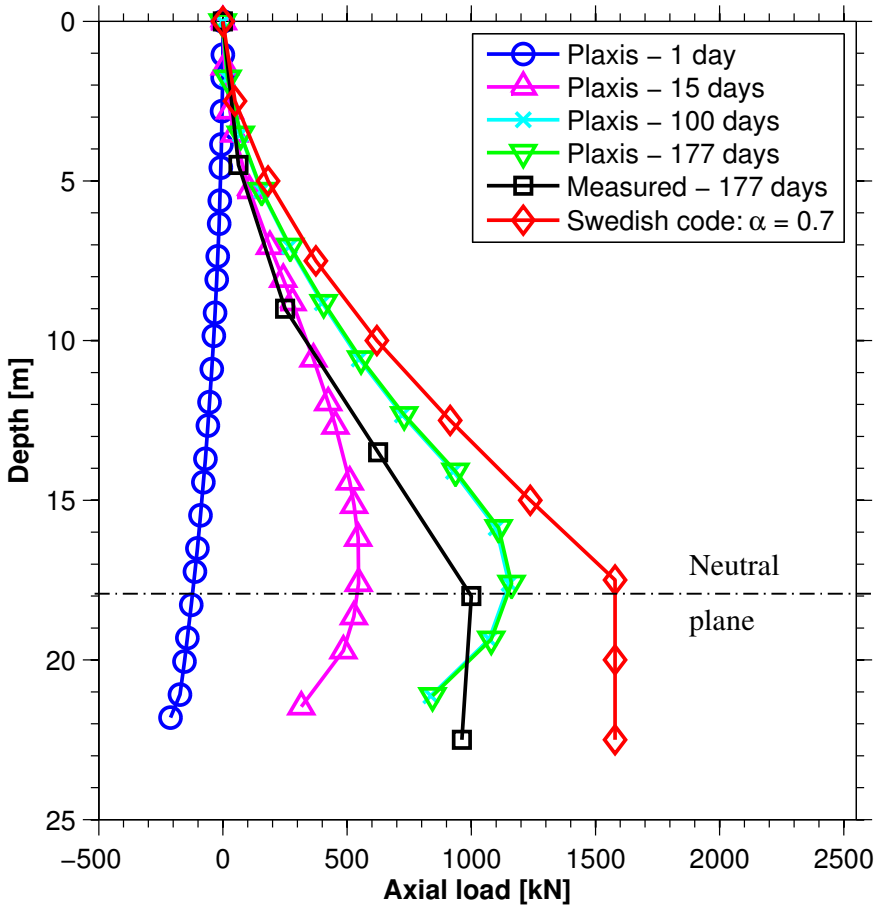

Figure 4.6: Comparison of axial loads calculated from PLAXIS and the α-method according to Swedish practice with the measured axial loads.

4.2.4 Pile-soil settlements in Plaxis

The neutral plane is raised to 18 m depth after 15 days, see Figure 4.7. This is close to the location of the measured maximum axial load in Figure 4.6.

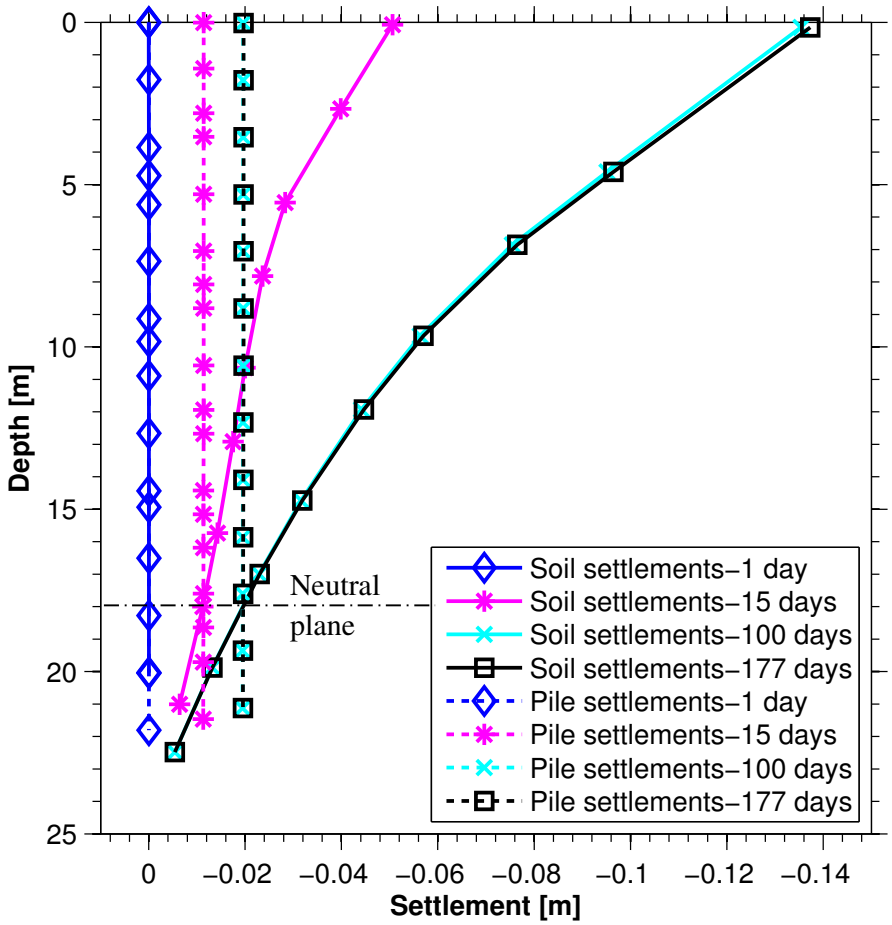

Figure 4.7: PLAXIS calculated ground settlement profiles (5 m away from the pile) and pile settlement profiles

4.2.5 Excess pore water pressure

Maximum excess pore water pressure of about 4.0 kPa is observed after the water table is lowered by 0.4 m (i.e. after one day). On fully lowering the water table by 6 m, the excess pore water pressure reaches a maximum of 44 kPa. Final excess pore water pressure is less than 5 kPa, see Figure 4.8.

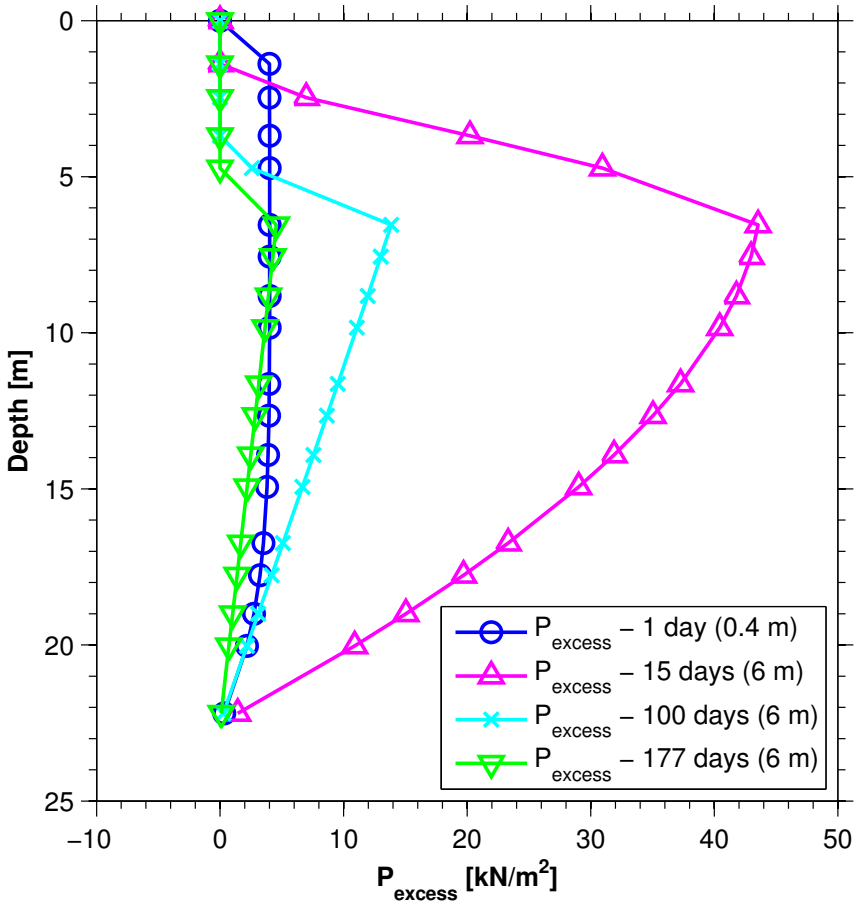

Figure 4.8: PLAXIS calculated excess pore water pressure 10 m away from the pile (Groundwater depths shown in brackets)

4.2.6 The α-factor

The value of the α-factor increases with time due to increased effective stresses and mobilized shear as a result of consolidation. The α-factors above the neutral plane are in the range of 0.4-0.6 at the end of consolidation. The α-factor in this case is lower than α of 0.7 used in Swedish practice to estimate negative skin friction and axial loads in Figure 4.5 and Figure 4.6. Negative α-factors indicate positive shaft resistance, which is observed during the first day and also below the neutral plane.

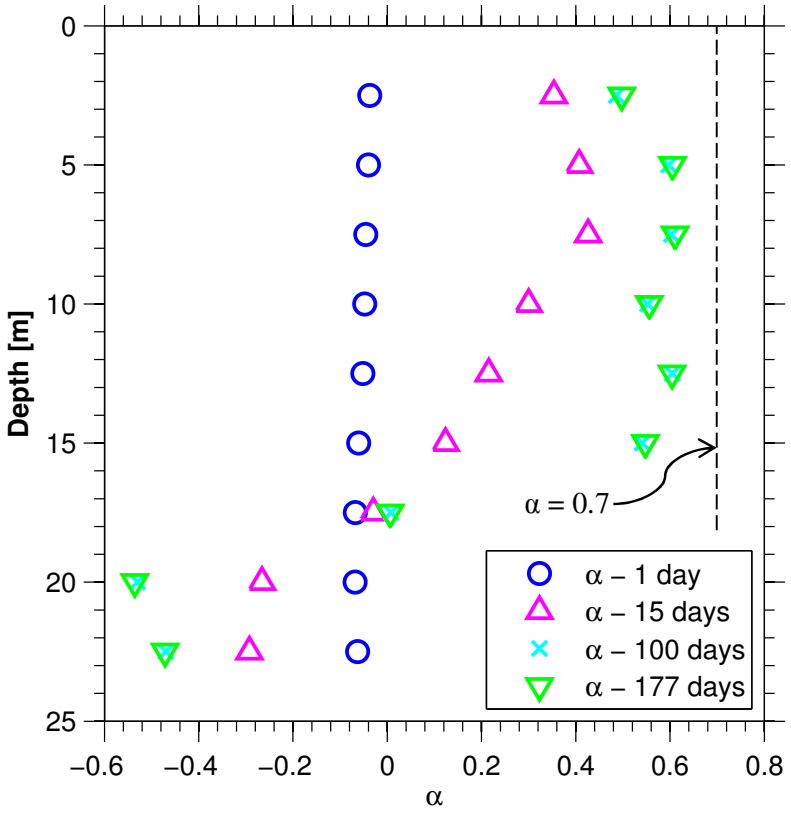

Figure 4.9: Variation of α factor at different stages of consolidation (α =mobilized shaft shear/initial undrained shear strength simulated from a PLAXIS triaxial test)

4.3 Parameter study

A parameter study is carried out to find which parameters have the greatest influence on skin friction mobilized at the pile-soil interface. The parameters are: interface roughness, pile diameter, pile stiffness and axial loads. A pile of diameter 300 mm and 22.5 m long is used. Other soil and pile properties are the kept the same as in the pile test.

4.3.1 Interface strength

The skin friction and axial loads increases and decreases in proportion with the change in interface strength reduction factor (see figure 4.10). The location of the neutral plane remains unaffected. This implies that the pile-soil settlements are not affected by the strength of the interface in the simulation, refer to Figure 4.10.

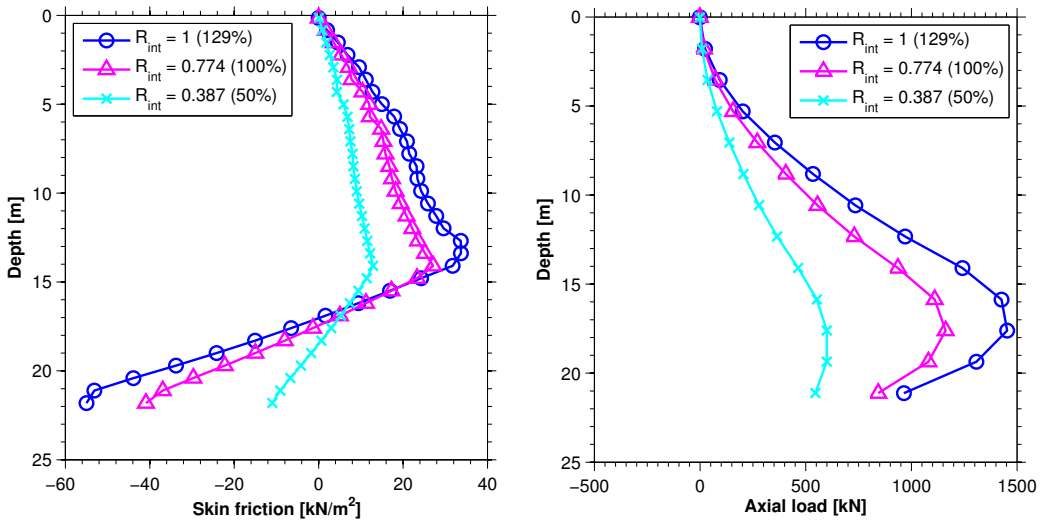

Figure 4.10: Influence of R_{int} on negative skin friction and axial loads

4.3.2 Pile stiffness

The stiffness of the pile has no influence on shaft friction within the investigated values of between 25.10^6 and 200.10^6 kPa. The pile is much stiffer relative to the soil and the drag loads from negative skin friction do not lead to large pile compression, see Figure 4.11.

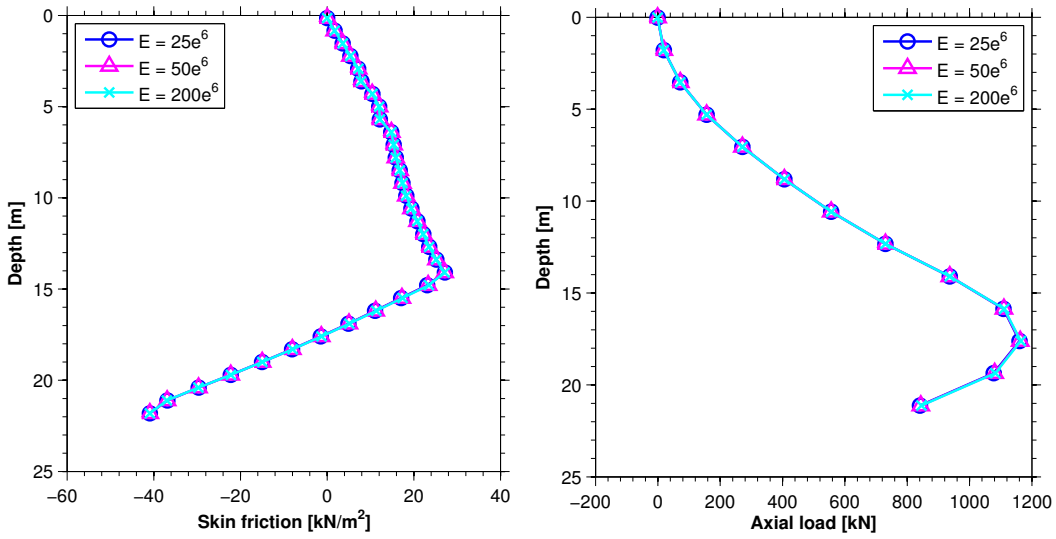

Figure 4.11: Effect of pile stiffness on skin friction and drag load

4.3.3 Pile diameter

There is a negligible effect of pile diameter on the negative skin friction. The difference in drag loads is expected due to differences in pile shaft surface area which varies with pile diameter, refer to Figure 4.12.

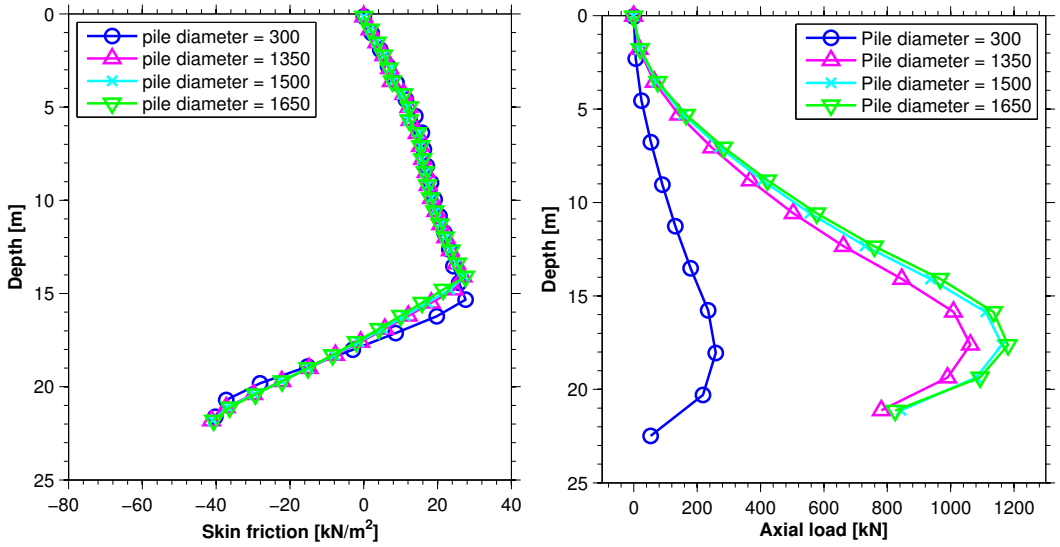

Figure 4.12: Effect of pile diameter on skin friction and axial load

4.3.4 Axial loads

Application of axial loads reduces negative skin friction, see Figure 4.13. The negative skin friction is eliminated after a force of 500 kN is applied. The pile head settlements at 250 kN, 500 kN and 1000 kN was 26, 33 and 73 mm an increment from 20 mm (for the case without axial loads in Figure 4.7).

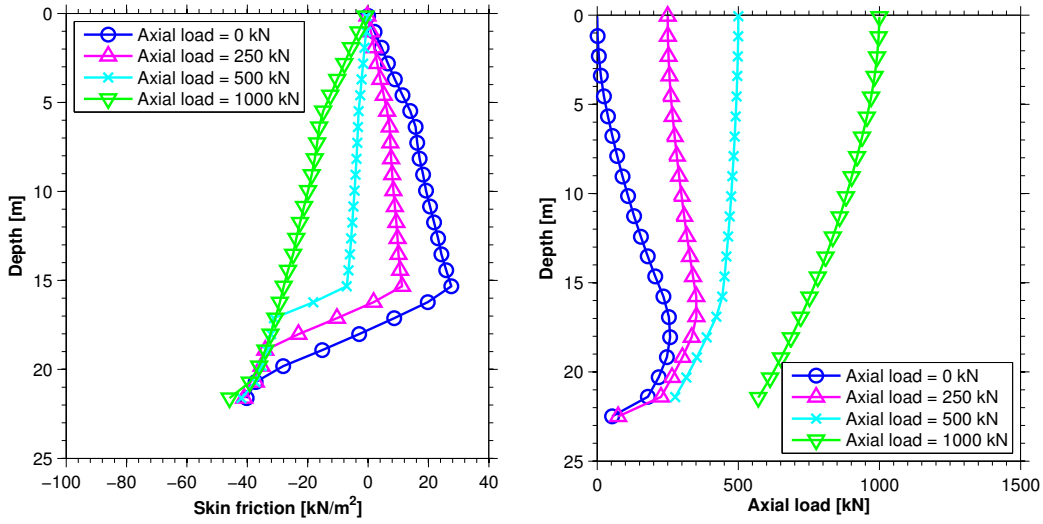

Figure 4.13: Effect of axial loads on skin friction and axial load

4.4 Discussion

Geotechnical centrifuge modelling is one of the ways to investigate soil structure interaction problems in geotechnical engineering. It was noted in Section 3.2.1 that there are problems experienced due to the scaling of the pile relative to the soil particles (where the average soil particles size remain constant in model and prototype). In this reference test, the ratio of model pile diameter to the average grain size is likely to be large because of the relatively small particles of silty clay (D_{10} = 0.003 mm). This implies that problems regarding scaling effects are small (Lundberg et al., 2012).

Modelling a pile in PLAXIS 2D axisymmetric environment limits analysis to piles with a circular cross section. It is therefore not possible to study pile groups and other pile shapes.

The initial stress generation by automatic calculation of K_0 failed to generate reasonable horizontal stresses and the soil surface developed plastic points (failure). Hence a K_0 for each layer was manually calculated. The Soft Soil model does not capture well the deformation in the top layer which is highly over-consolidated. In natural clay soil profiles, for example in Scandinavia, this top layer (usually varies from 1-5 m of top soil) consists of desiccated crust due to exposure to drying, freezing, leaching and oxidation.

Modelling the sand layer with the estimated stiffness of 20, 000 kPa gives axial forces closer to the measured result. The profile of skin friction is different from the measured result. It is a possibility that the pile may have penetrated into the sand. The author of the test acknowledges that although the pile was intended to have a fixed base, pile movement occurred at the pile toe (Lee et al., 2002). There are uncertainties remaining in this aspect which are not possible to properly include in the model as those are not reported in experimental test data.

The output of the PLAXIS model overpredicted the measured axial load by 17 %. The final ground settlements were underestimated by 35%. The effect from creep is expected to be negligible due to the short test duration (less than 2 hours in a geotechnical centrifuge). There could have been some differences in excess pore pressure at the end of consolidation but since the results of pore pressure were not presented, a comparison of excess pore pressure has not been carried out.

The calculation of negative skin friction using an α-factor of 0.7 overestimates the drag loads by 76%. A maximum long-term α-factor of 0.6 is obtained from the numerical analysis and is in the range for bored piles discussed earlier in Section 2.2.1 of between 0.3 and 1. It is less than α-factor of 0.7 that is recommended in Sweden. This difference may be due to differences in soil properties between the tested soil and that which was used to back figure the Swedish α-factor of 0.7.

The diameter of the pile and the stiffness of the pile material least affected the result of skin friction. The axial loads reverse the interface shear stresses as they cause the

pile to settle more than the soil. This removes negative skin friction, but the settlements and pile axial forces may exceed set criteria for design. For the analysed pile, settlements of 73 mm were recorded as a result of application of 1,000 kN axial load as a result of compression of the sand layer. The parameter R_{int} has been found to have a big influence on the magnitude of skin friction mobilized at the interface.

5 CONCLUSION AND RECOMMENDATIONS

5.1 Conclusion

A numerical simulation of the mobilisation of negative skin friction due to the lowering of the groundwater table has been carried out. The experimental data is retrieved from a well-documented geotechnical centrifuge test. The numerical simulations are performed with PLAXIS and the build in Soft Soil constitutive model. The pile axial loads overpredicted the measured result with 17%. The result could potentially have been improved if more information on the test was available such as the soil properties, excess pore water pressure generation and the condition of pile support at the pile toe.

To model the deformations better, the highly overconsolidated top layer should be modelled as an elastic material in real soils profiles, for example by using the Mohr-Coulomb model in PLAXIS.

The analytical calculation with α-factor of 0.7 overestimated axial loads by 76%. Advanced numerical analysis, which is more expensive, is therefore recommended in projects where an optimized solution will bring savings over calculations obtained from empirical methods. In small projects, the savings from an improved solution may not pay off the resources invested in the numerical analysis e.g. in carrying out a detailed soil investigation.

The pile diameter and stiffness had negligible effect on pile axial loads, while the interface roughness and axial loads had a greater effect. This suggests that there is possibility to reduce negative skin friction on piles by smoothing the interface between soil and pile. Furthermore, it is essential to accurately capture the interface properties and pile-soil settlements in order to properly numerically model the distribution of skin friction and axial loads on a pile.

The simulation shows that maximum negative skin friction is achieved at the end of consolidation. Therefore, a design for worst case scenario may easily be estimated by carrying out a drained calculation.

This numerical analysis has been carried out with few uncertainties. In a real design scenario, the ground is more heterogeneous and it is more difficult to properly determine boundaries for example those of groundwater flow and initial pore pressures. A detailed site investigation to obtain the representative soil properties is important to get high quality results from a full numerical analysis such as those presented here. When using finite element methods (FEM) to analyse a pile, it is important to compare FEM output with regular calculation methods and also use engineering judgement and experience to ensure the output is within reasonable range.

5.2 Recommendations for future work

More research is recommended on full scale piles. Modelling of pile groups also needs be investigated. It will also be interesting to find out how the interaction between the piles in a pile group affects negative skin friction. The effect of creep also needs to be researched by using a more advanced soil model such as the Soft Soil creep model. Future analysis should also consider analysing piles as 3D elements.

References

Boulon, M., Garnica, P. & Vermeer, P.A., 1995. *Soil-structure interaction: FEM computations*. Elsevier Science B.V.

Bowles, J.E., 1997. *Foundation analysis and design*. Singapore: McGraw Hill.

Briaud, J.L., 2013. *Introduction to geotechnical engineering*. New Jersey: John Wiley & Sons.

Brinkgreve, R.J.B., 2014. *Pile modelling in a 2D plain strain model*. [Online] Available at: http://kb.plaxis.com/tips-and-tricks/pile-modelling-2d-plain-strain-model [Accessed 21 January 2015].

Brinkgreve, R.J.B., Engin, E. & Swolfs, W.M., 2014. *Material model manual*.

Brinkgreve, R., Leoni, M. & Marcelo, S., 2014. *Numerical modelling: critical state models*. [Pdf lecture notes] Gothenburg Available at: http://pingpong.chalmers.se/ [Accessed 14 March 2015].

Davison, M.T., 1993. Negative Skin Friction in Piles and Design Decisions. In *Third International Conference on Case Histories in Geotechnical Engineering*. Missouri, 1993.

Erikson, P., Jendeby, L., Olsson, T. & Svensson, T., 2004. *Cohesion piles*.

Fellenius, B.H., 1998. Recent advances in the design of piles for axial loads, dragloads, downdrag, and settlement. In *ASCE and Port of NY & NJ Seminar.*, 1998.

Fellenius, B., 2006. Results from long-term measurement in piles of drag load and downdrag. *Canadian Geotechnical Journal*, pp.409-30.

Fellenius, B., 2014. *Basics of foundation design*. Available at: http://www.fellenius.net/papers.html [accessed 23 January 2015].

Kempfert, H. & Gebreselassie, B., 2006. *Excavations and foundadtions in soft soils*.

Kezdi, A. & Rethati, L., 1988. *Handbook of soil mechanics*.

Knappett, J.A. & Craig, R.F., 2012. *Craig's soil mechanics*. Oxon: Spon press.

Lee, C.J., Bolton, M.D. & AL-Tabbaa, A., 2002. Numerical modelling of group effects on the distribution of dragloads in pile foundations. *Geotechnique* , 52, pp.325-35.

Lee, C.H. & Chen, C.R., 2003. Negative skin friction on piles due to lowering of groundwater table. *Journal of the southeast Asian geotechnical society*, pp.13-25.

Lee, C.J., Chen, H.T. & Wang, W.H., 1998. Negative skin friction on a pile due to excessive groundwater withdrawal. In *Centrifuge 98*. Rotterdam, 1998. Balkema.

Lundberg, B., Dijkstra, J. & Tol, V., 2012. *On the modelling of piles in sand in the small geotechnical centrifuge*. TU Delft.

Muir Wood, D., 2004. *Geotechnical modelling*.

Ng, C.W.W., 2013. The state-of-the-art centrifuge modelling of geotechnical problems at HKUST. *Journal of Zhejiang University-SCIENCE A*, pp.1-21.

Niazi, F.S. & Mayne, P.W., 2013. *Cone penetration test based direct methods for evaluating static axial capacity of single piles*. Springer.

Olsson, M., 2010. *Calculating long-term settlement in soft clays*. Göteborg: Chalmers.

Plaxis, 2013. *Plaxis 2D reference manual*.

Potts, D.M., 1999. *Finite element analysis in geotechnical engineering*. London : Thomas Telford.
Tomlinson, M. & Woodward, J., 2008. *Pile design and construction practice*. Oxon: Taylor & Francis.
Wong, K.S. & Teh, C.I., 1995. Negative skin friction on piles in layered soil deposits. *Journal of Geotechnical Engineering*, pp.457-65.

APPENDICES

Appendix A1: Interface (plastic analysis)

The properties of the concrete and soil are presented in Table 7.1.

Table 7.1: Properties of the block and the interface

Property	**Concrete block**	**Interface (soil)**	**Unit**
Material model	Linear elastic	Mohr coulomb	-
Drainage type	None-porous	Drained	-
Unit weight (γ)	24	0	kN/m^3
Stiffness (E)	$25e^6$	1,000	kN/m^2
Poisson ratio (v)	0.3	0.3	-
Internal friction angle (ϕ')	-	30	^{o}
Cohesion (c')	-	2	kN/m^2

The model is presented in Figure 7.1.

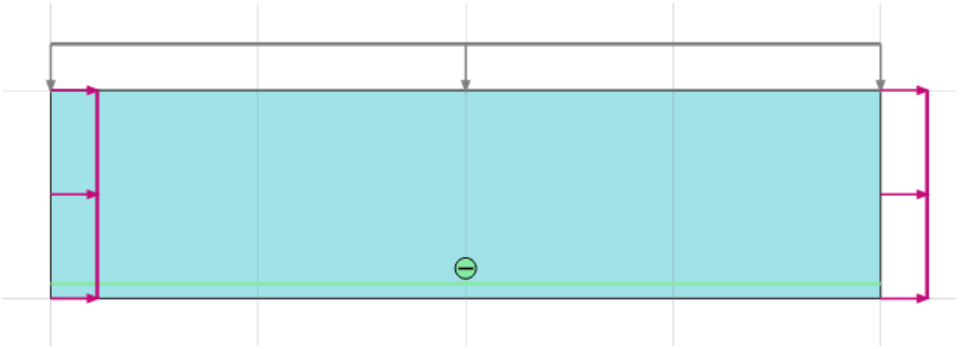

Figure 7.1: Model setup

The response of the interface to changes in interface roughness and normal loads is investigated and discussed below.

i) R_{int}

Figure 7.2 and shows that the average shear at the interface increases in direct proportion with increase in the interface coefficient (R_{int}). Figure 7.3 shows the result for $R_{int} = 1$.

The average maximum stress at the interface can be estimated using Equation 7.1:

$$\tau_{max} = R_{int}.c' + \sigma'_n.R_{int}.tan(\phi') \quad (7.1)$$

$$= 2 + 24 * tan(30) = 15.86\ kN/m^2$$

From the simulation, R_{int} of 1 gives an average shear stress of 15.87 kN/m^2 (see Figure 7.3) which is approximately equal to that estimated using Equation 7.1 above.

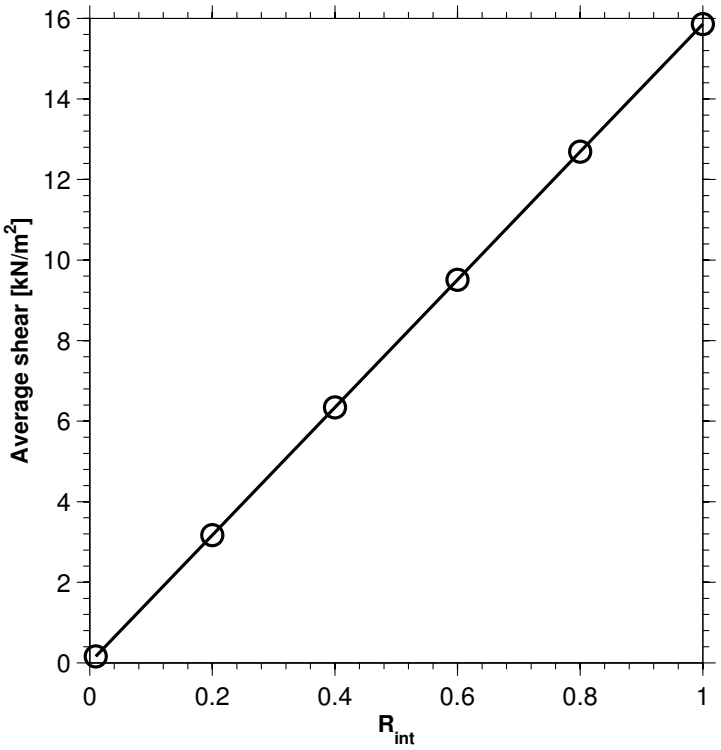

Figure 7.2: Plot of average shear against interface coefficient, R_{int}

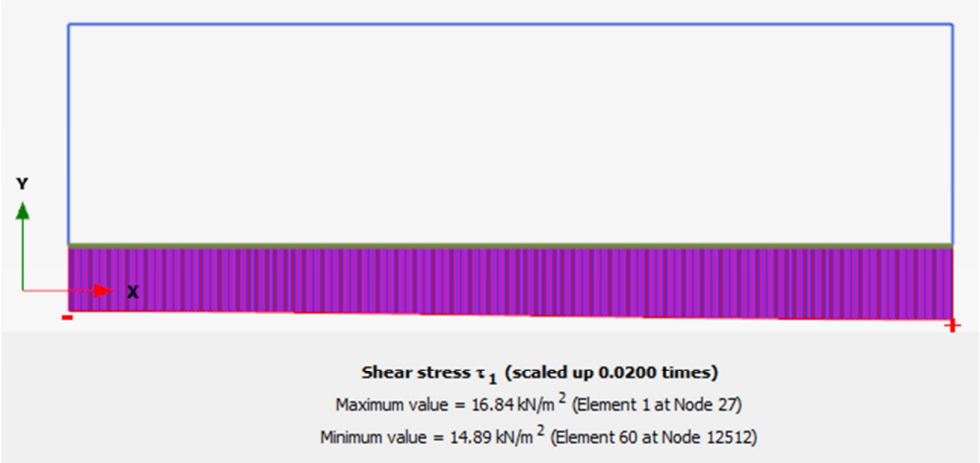

Figure 7.3: Shear stress distribution at R_{int} of 1

ii) Normal loads

The Figure 7.4 illustrates the relationship between shear and normal stress. The trend shows an increase of shear with increase in normal stress. Lower interface strength reduction factor R_{int} results in a low shear interface shear as expected. The shear at zero normal loads which is not expected is due to the self-weight of the concrete block.

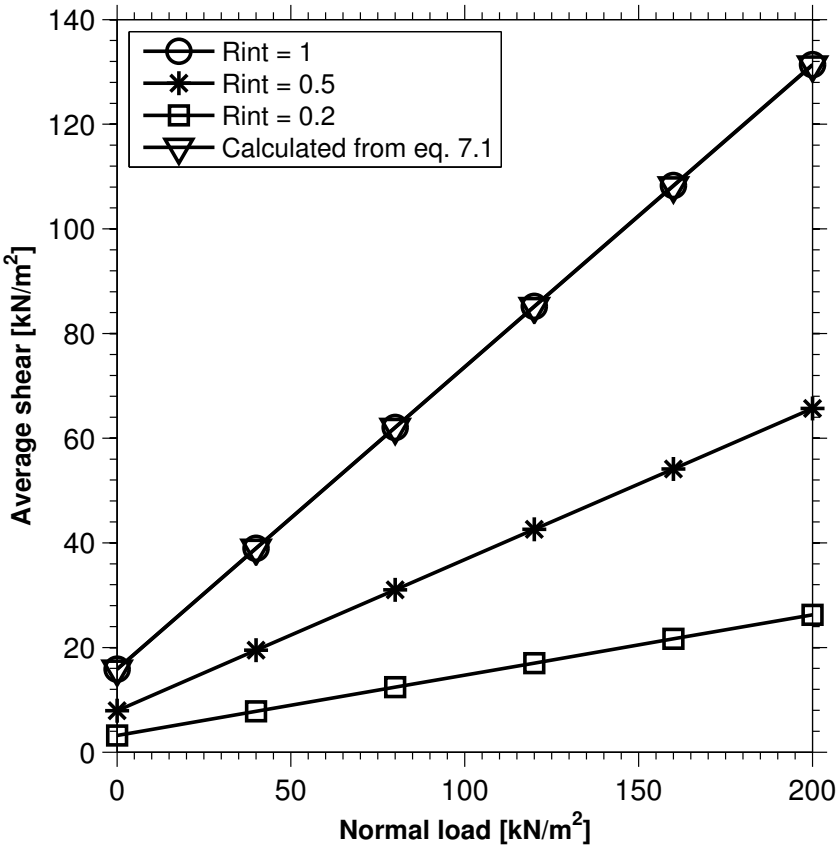

Figure 7.4: Plot of average shear against normal loads for R_{int} = 0.2, 0.5 and 1; and a plot of Equation 8.1.

Appendix A2: Interface plastic and consolidation analysis

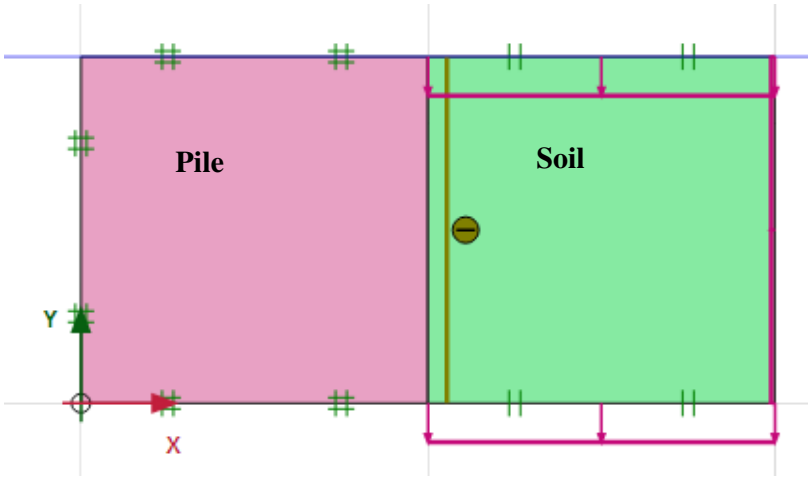

Figure 7.6: Model setup

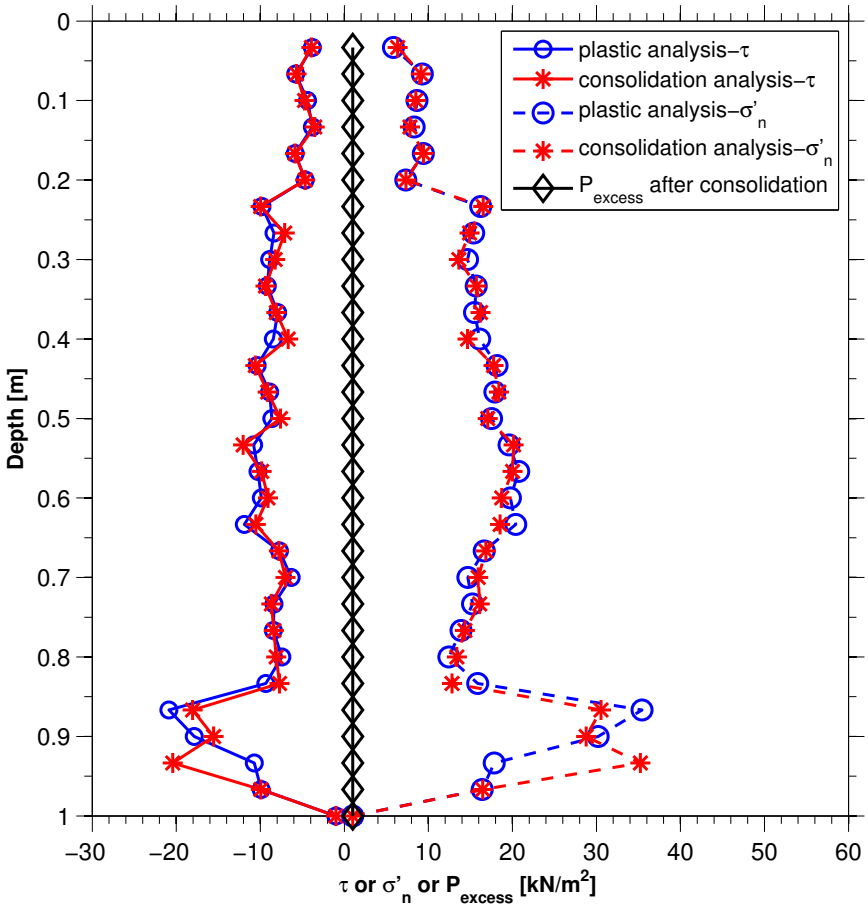

Figure 7.7: A comparison between drained analysis and long term consolidation analysis

Appendix A3: Estimating the initial void ratio

Table 7.2: Estimating the initial void ratio using an effective overburden of 155 kN/m^2 at 22.5 m depth.

Parameter	**Value**	**Unit**
Gravity, g	9.81	m/s^2
Relative soil density, Gs	2.65	kN/m^3
Specific unit weight [(a)]	26.00	kN/m^3
Density of water, Υ_w	9.81	kN/m^3
Depth (saturated soil), d	22.50	m
Effective overburden, σ'_{vo}	155.00	kN/m^2
Submerged soil unit weight [(b)]	6.89	kN/m^3
Saturated density, Υ_{sat} [(c)]	16.70	kN/m^3
Volume of solids [(d)]	0.43	
Volume of voids [(e)]	0.57	
Void ratio, e	1.35	

Note

a) Specific unit weight = G_s. g

b) Submerged soil unit weight = σ'_{vo}/h

c) Υ_{sat} = Submerged soil unit weight + Υ_w

d) Volume of solids = Submerged soil unit weight /(Gs - Υ_w)

e) Volume of voids = 1 - volume of solids.

Appendix A4: OCR and undrained shear strength

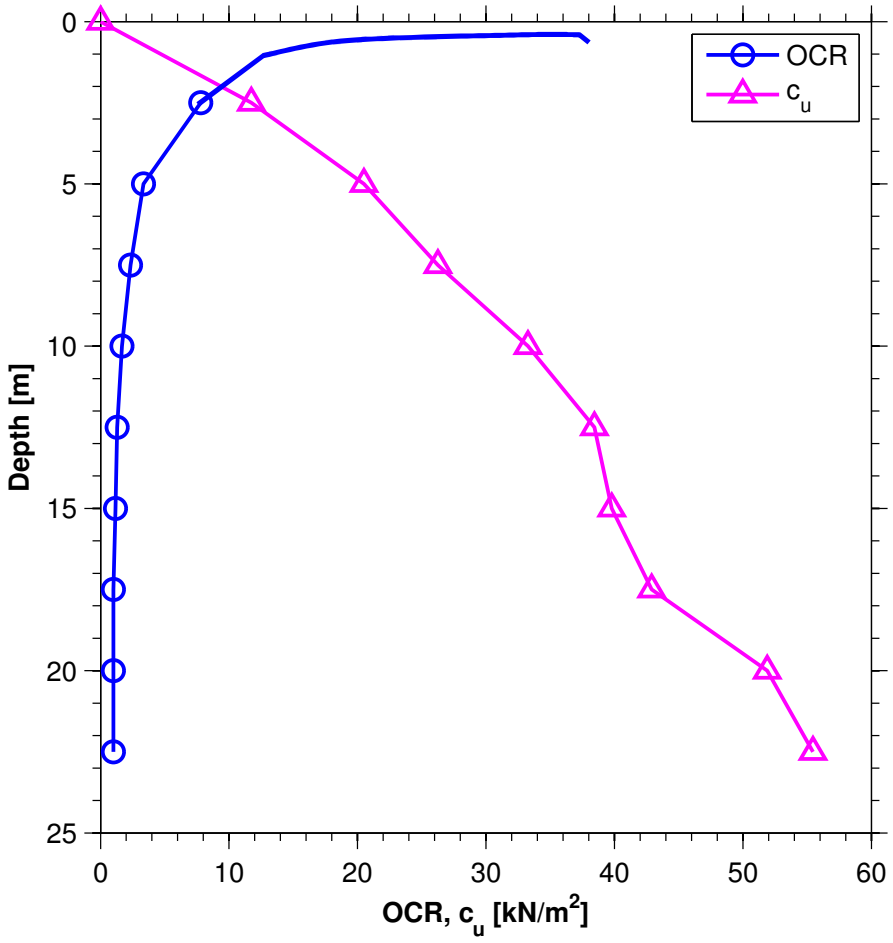

Figure 7.8: Variation of OCR and undrained shear strength (c_u) with depth (c_u is simulated from undrained triaxial test)

Appendix A5: Final soil settlement profiles

The soil settlement is estimated using 1D consolidation equations for estimating negative skin friction using an α-factor of 0.7:

$$S = \frac{C_s.H.\log\left(\frac{\sigma_2}{\sigma_1}\right)}{1+e_0} \qquad \text{for } \sigma_1<\sigma_2 < p_c$$

$$S = \frac{C_c.H.\log\left(\frac{p_c}{\sigma_1}\right)}{1+e_0} + \frac{C_s.H.\log\left(\frac{\sigma_2}{p_c}\right)}{1+e_0} \qquad \text{for } \sigma_1<p_c < \sigma_2$$

$$S = \frac{C_c.H.\log\left(\frac{\sigma_2}{\sigma_1}\right)}{1+e_0} \qquad \text{for } p_c<\sigma_1 < \sigma_2$$

where σ_1, σ_2 and $p_c$are initial stress, final stress and preconsolidation pressure respectively. S is sub-layer settlement, H is the height of each soil sub-layer and e_0 is the initial void ratio.

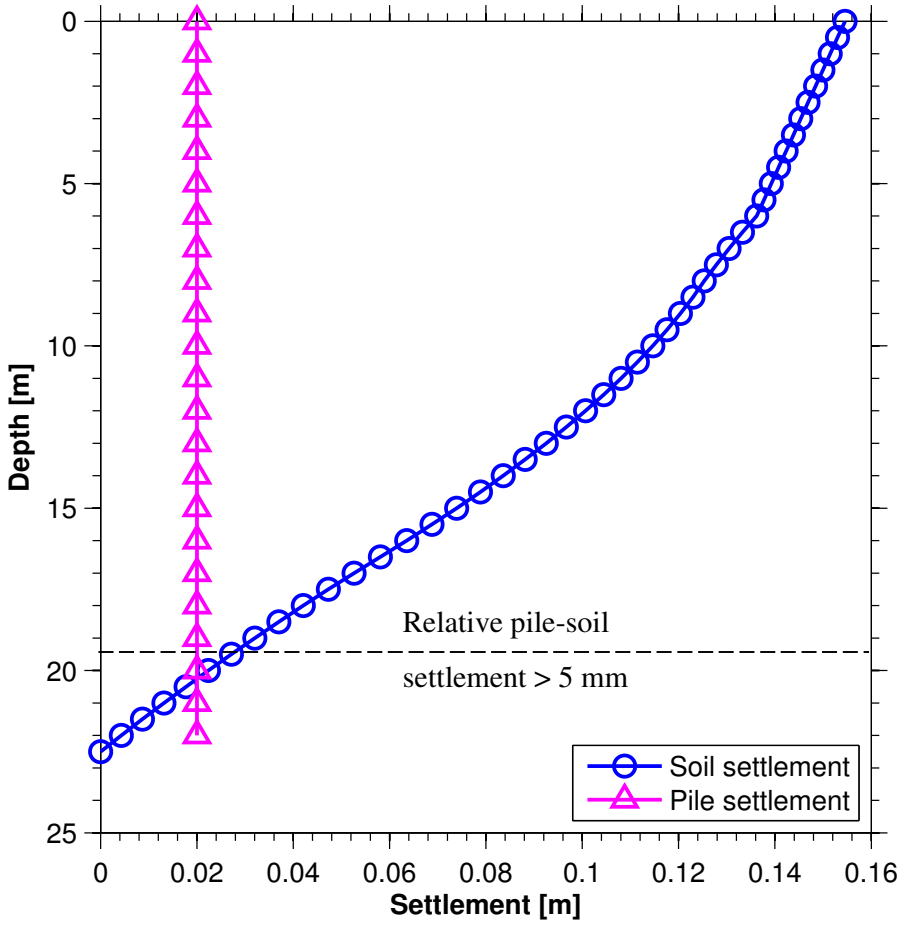

Figure 7.9: Calculated soil settlements from 1-D consolidation